JOURNAL OF GUIDANCE, CONTROL, AND DYNAMICS
Vol. 33, No. 6, November–December 2010

Engineering Notes

Output Regulation with Actuator Saturation for the Benchmark Active Control Technology Model

Ellen Applebaum,* Zvi J. Adin,† and Joseph Z. Ben-Asher‡
Technion–Israel Institute of Technology, Haifa 32000, Israel

DOI: 10.2514/1.45668

I. Introduction

DURING the past several years, flutter suppression techniques have been actively investigated on the Benchmark Active Control Technology (BACT) wind-tunnel aeroservoelastic (ASE) model developed by NASA Langley Research Center [1–7]. The BACT exhibits classical flutter instability at transonic speeds, with system dynamics that vary with the dynamic pressure. The BACT has provided a testbed for the development and testing of passivity-based robust control, linear parameter varying gain scheduling control, *H*-infinity μ-synthesis generalized predictive control, full-order and reduced-order linear quadratic Gaussian (LQG), and others. The body of flutter suppression techniques developed for the BACT model is based upon a system that can be effectively reduced to a low-order state-space model. The open-loop BACT model has one flutter mechanism; it is stable below the classical flutter boundary, and it is unstable above [2].

This Note addresses the problem of output regulation of the continuous-time linear BACT model with control saturation and exogenous input additive disturbance. The motivation for this Note is a previous study on flutter suppression of a generic high-order nonminimum-phase unmanned aerial vehicle system using a piezoelectric aileron with restricted control authority [7].

A chronological bibliography of research that addresses control with saturating actuators is reported in [8]. There are generally two approaches for dealing with actuator saturation. In the first approach, one starts with the control design and then adds problem-specific schemes, referred to as antiwindup schemes, which use ad hoc modifications for dealing with control saturation. Classical methods of control law design for flutter suppression of the BACT system have tended to use this approach. Optimization methods, such as min-max and state-dependent Riccati equation methods, have also been applied to flutter suppression with hard constraints on the control input [3,9]. Both methods require validation of controllability and stability for specific initial conditions and control constraints through an iterative process of parameter selection and numerical simulations. The second approach is the one addressed in this Note. It takes into account the saturation nonlinearity at the outset of the control law design in a systematic manner that provides semiglobal stabilization of system dynamics.

Previous work by Applebaum and Ben-Asher on flutter suppression of the BACT wind-tunnel model, subject to bounded control signals, described the theory and results for estimating domains of attraction of the origin that approach the system's null controllable region [10] and for constructing a continuous dynamic state-feedback saturated control law that guarantees stability on a predefined subset of the domain of attraction in the presence of exogenous disturbance [11]. This Note extends these results to the construction of a dynamic output error-feedback regulator. It is based upon the work of Hu and Lin [12,13] that provided a general theoretical framework for output regulation with control saturation. Output regulation of the BACT model, using both state and output error feedback, is demonstrated through simulations that have been carried out for the highest considered dynamic pressure value, corresponding to the system's most open-loop unstable working setpoint.

An alternative approach to the stabilization of systems with saturating actuators includes the application of linear-quadratic-regulation (LQR)/LQG theory and stochastic approximations for dealing with control saturation [14]. In contrast with the stochastic approximation method, this study provides a precise methodology for achieving stabilization of the BACT model under saturation control. State-feedback stabilization of linear unstable plants with saturating actuators using a time-varying sliding surface has also been proposed as a robust stabilization method for single-input/single-output (SISO) systems containing nonsmooth nonlinearities such as saturation [15]. This study proposes an alternative strategy and methodology to that of sliding mode control for achieving output regulation of a linear system with actuator saturation and exogenous disturbances. This method is based upon the construction of invariant sets for maximizing domains of attraction and achieving continuous control action in small invariant neighborhoods of the equilibrium point.

The organization of the Note is as follows. Section II presents a general description of the output regulation problem. Section III offers a brief description of the BACT model. Section IV presents some preliminary concepts. These include a description of the canonical modal transformation of the BACT system and a mathematical description of the stabilizing state-feedback control law that forms the nucleus of the dynamic control law design. The definitions of null controllable and asymptotically regulatable regions are also presented in this section. One design goal is the formation of domains of attraction within a sufficiently large subset of the regulatable region. Section V addresses this goal by presenting theorems on invariant sets and the method for the construction of an invariant set that will be used subsequently in control law design. Section VI presents the algorithm for dynamic state-feedback control. The output regulation control law is extended in Sec. VII to the practical real-world case of output regulation with dynamic error feedback. Section VIII presents a numerical example based upon the worst-case open-loop dynamics of the BACT model. Numerical simulations demonstrate the sensitivity of the error-feedback control law to the frequency content of the external persistent disturbance, relative to the system aeroelastic resonance frequency. Additionally, this section addresses the robustness of the state-feedback and error-feedback control laws, synthesized for the nominal worst-case open-loop dynamics and subject to variations in the airflow dynamic pressure of open-loop BACT plants and to unmodeled perturbations of the external frequency content. The conclusions of Sec. IX summarize the main results of this study and suggest directions for further research.

II. Problem Statement

This section summarizes the formulation of the problem of output regulation with bounded control. It is based on the classical formulation and results regarding the problem of output regulation

Received 26 May 2009; revision received 17 March 2010; accepted for publication 17 March 2010.

*Research Scientist, Faculty of Aerospace Engineering, Technion.
†Aerospace Engineer, Rafael Advanced Defence Systems, Ltd., Missile and Control Department, Missile Division, Haifa, Israel.
‡Professor, Faculty of Aerospace Engineering. Associate Fellow AIAA.

for linear systems [16]. Consider the following linear system:

$$\dot{\mathbf{x}} = A\mathbf{x} + Bu + \mathcal{P}\mathbf{w}, \qquad \dot{\mathbf{w}} = S\mathbf{w}, \qquad e = C\mathbf{x} + Q\mathbf{w} \tag{1}$$

The first equation of the system in Eq. (1) describes a plant with state $\mathbf{x} \in R^n$ and input $u \in R^m$, subject to a disturbance represented by $\mathcal{P}\mathbf{w}$. The second equation describes the exosystem with system matrix S for modeling the class of disturbances and references with state $\mathbf{w} \in R^r$. The third equation describes the error e between the actual plant output $C\mathbf{x}$ and a reference signal $-Q\mathbf{w}$. In the study of the BACT system, it is assumed that $Q = 0, n = 8, m = 1, r = 2$, and $e = C\mathbf{x} \in R^1$.

It is well known that, under mild assumptions [13,16,17], the output regulation problem in Eq. (1) is solvable if, and only if, there exist matrices Π and Γ that solve the linear matrix equations

$$\Pi S = A\Pi + B\Gamma + \mathcal{P}, \qquad C\Pi + Q = 0 \tag{2}$$

Given these mild assumptions, the following state transformation is used to transform the output regulation problem into a stabilization problem: let $\mathbf{z} = \mathbf{x} - \Pi\mathbf{w}$. Then $\dot{\mathbf{z}} = \dot{\mathbf{x}} - \Pi\dot{\mathbf{w}}$ and, by making appropriate matrix equation substitutions, the system in Eq. (1) can be rewritten as

$$\dot{\mathbf{z}} = A\mathbf{z} + Bu - B\Gamma\mathbf{w} \qquad \dot{\mathbf{w}} = S\mathbf{w} \qquad e = C\mathbf{z} \tag{3}$$

The output regulation of the linear system in Eq. (3) is subject to control constraint u, belonging to the set of all admissible controls $\mathcal{U}$, where $\mathcal{U} = \{u \in R^m\colon u \text{ is measurable, and}$

$$|u(t)|_\infty = \max_i |u_i(t)| \le 1, \quad \forall\ t \in R\} \tag{4}$$

The set $\mathcal{U}$ is a compact convex set with the origin in its interior. For a given scalar δ, define the set

$$\delta\mathcal{U} = \{\delta u\colon u \in \mathcal{U}\}$$

From the convexity of set $\mathcal{U}$ [13], if $\delta \in [0, 1]$, $u_1 \in \delta\mathcal{U}$ and $u_2 \in (1 - \delta)\mathcal{U}$, then $u = u_1 + u_2 \in \mathcal{U}$.

This property of $\mathcal{U}$ is used in the construction of dynamic feedback laws satisfying the solution criteria of the output regulation problem in Eq. (3). The control action $u(\cdot)$ can be provided either by state feedback or by output-tracking error feedback. The following are necessary assumptions on the plant and exosystem [13]:

1) The system of matrix equations (2) has a solution (Π, Γ).

2) The matrix S has all its eigenvalues on the imaginary axis and is neutrally stable.

3) The pair (A, B) is stabilizable.

4) The initial state $\mathbf{w}_0$ of the exosystem is in the set

$$\mathcal{W}_\mathbf{0} = \{\mathbf{w}_0 \in R^r\colon \Gamma e^{St}\mathbf{w}_\mathbf{0} \in \hat{\rho}\mathcal{U}, \quad \forall\ t \ge 0\} \tag{5}$$

for some $\hat{\rho} \in [0, 1)$ and $\mathcal{W}_0$ compact. Denote $\delta = 1 - \hat{\rho}$. The parameter δ is used in the construction of the dynamic output regulation control law. The solution trajectory of the exosystem is $\mathbf{w}(t) = e^{St}\mathbf{w}_\mathbf{0}$. It follows that $\Gamma\mathbf{w}(t) \in \hat{\rho}\mathcal{U} = (1 - \delta)\mathcal{U}\ \forall\ t \ge 0$ and, by definition of $\mathcal{U}$, $|\Gamma\mathbf{w}|_\infty \le \hat{\rho}$.

Consider the connection of the system in Eq. (3) to a dynamic output regulation control law:

$$u = g(\alpha, \mathbf{z}, \mathbf{w}), \qquad g(\alpha, \mathbf{z}, \mathbf{w}) \in \mathcal{U}, \qquad \dot{\alpha} = h(\alpha, \mathbf{z}, \mathbf{w})$$
$$\alpha(0) = \alpha_0 \tag{6}$$

where h and g are continuous real-valued functions,

$$\alpha = \begin{bmatrix} \alpha_1 \\ \alpha_2 \end{bmatrix} \in R^2$$

and α_0 is the initial value of α.

For the regulation problem in Eq. (3), the objective is to achieve internal stability and output regulation. A feedback control action $u = f(\mathbf{z})$ achieves internal stability when the closed-loop system with a zero-additive disturbance, disconnected from its exosystem, is asymptotically stable. Output regulation is achieved when, for any initial condition $(\mathbf{z}_0, \mathbf{w}_0)$ of the plant and exosystem, the state $\mathbf{z}(t)$ of the plant is bounded and, for any initial state $(\mathbf{z}_0, \mathbf{w}_0)$, sufficiently close to the origin, $e(t) \to 0$ as $t \to \infty$. The system in Eq. (3) is said to be solvable when a dynamic controller u in Eq. (6) exists for which the system achieves internal stability and output regulation. The focus of this study is on the existence of solutions for system (3), connected to a dynamic controller u, that satisfies the following criteria: 1) trajectories that begin in an a priori-defined invariant set remain bounded, and 2) the output error e converges asymptotically to zero in an a priori-defined local invariant neighborhood of the origin.

III. Benchmark Active Control Technology Model

The BACT wind-tunnel model is a rigid rectangular wing, with a NACA 0012 airfoil section, equipped with a trailing-edge (TE) flap control surface [2,3,14]. The wing is attached to a flexible mount system that allows two rigid-body degrees of freedom: vertical plunge displacement and pitch angle. The TE flap angle of deflection is actuated via an electrical servomotor, for which the voltage input serves as the system control input. The wing's vertical acceleration measurements are used for feedback control. In this study, a single accelerometer is located at the wing shear center. The BACT model's ASE dynamic response varies with the airflow dynamic pressure q. In this study, it is modeled as a low-order SISO linear dynamic system with the following state-space realization and with dynamic pressure-dependent coefficients:

$$\dot{\mathbf{x}}^b = A(q)\mathbf{x}^b + B(q)u^b \qquad y^b = C(q)\mathbf{x}^b \tag{7}$$

where

$$\mathbf{x}^b \in R^8\text{-state vector} \qquad u \in R^1\text{-scalar control input}$$
$$y \in R^1\text{-scalar output}$$

The first four states represent the wing's vertical displacement and pitch angle (x_1^b and x_2^b) and generalized velocities (x_3^b and x_4^b). The fifth coordinate (x_5^b) models the aerodynamic state. The last three states (x_6^b–x_8^b) model the third-order wing-flap electrical actuator dynamics (which are invariant to the air flow dynamic pressure). The entries of the BACT system matrices $A(q)$, $B(q)$, and $C(q)$ were evaluated using ZAERO software [18] for 24 air-density discrete values ranging from 5×10^{-5} to 4×10^{-3} slug/ft^3 at a constant air flow velocity of 390 ft/s at Mach number 0.77. The dynamic

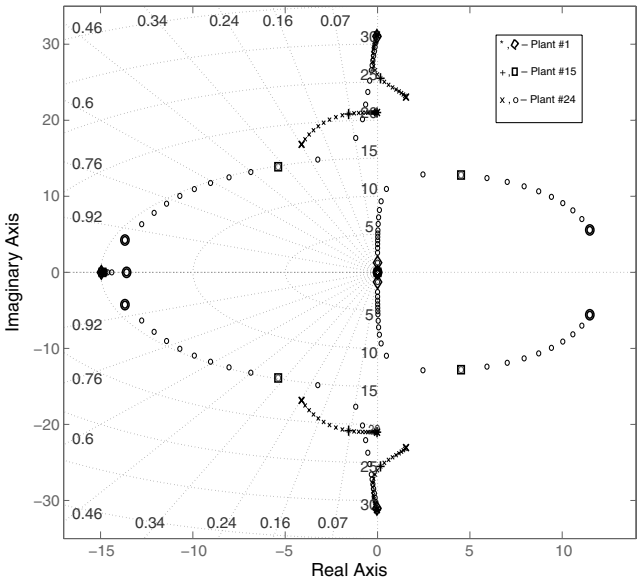

Fig. 1 BACT open-loop dynamic model transfer function dominant poles (×) and zeros (○) locations, as a function of the airflow dynamic pressure.

pressure varies from 548 psi (plant 1) to 43,805 psi (plant 24). For low dynamic pressure values, the system is open-loop stable; it gradually becomes unstable as the dynamic pressure increases. Flutter instability occurs for the first time at a dynamic pressure value of 24,093 psi, corresponding to plant 15. A conjugate complex pair of poles gradually moves to the right of the complex plane. This Note focuses on synthesizing a bounded control state feedback and an output-tracking error-feedback regulator for the BACT system's most open-loop unstable working point, plant 24.

The BACT system is linearly controllable, and hence stabilizable, for each pointwise constant dynamic pressure value. It is also a nonminimum phase system, having a right-hand conjugate complex pair of zeros, for which the real values increase with the airflow dynamic pressure.

Figure 1 depicts the root locus mapping of the BACT open-loop linearized dynamic model transfer function's dominant poles (denoted by x) and zeros (denoted by o) as a function of airflow dynamic pressure.

In addition, the wing-flap servomotor dynamic model has a unity dc gain, with three invariant high-bandwidth stable poles located at $-100, -92.6 \pm 137.0j$. Actual wing-flap servoactuators are usually subject to simultaneous bounds on their output hinge moment, rate of deflection, and effective bandwidth. In the case of the BACT system under study, we consider bounds only on the control magnitude: namely, on the actuator hinge moment bounds. Strict bounds on actuator output rate, or its effective bandwidth, are eventually bounds on the dynamic model's intermediate states, and their consideration is beyond the scope of this Note. Stabilization of dynamic systems subject to such additional actuator constraints are treated, for example, in chapter 14 of [12] and in [19,20].

IV. Preliminaries

The method of construction of continuous feedback laws for BACT is based upon the fact that the nth-order ($n = n_1 + n_2$) plant model has a second-order ($n_1 = 2$) antistable subsystem A_1 consisting of a pair of complex eigenvalues and a stable sixth-order ($n_2 = 6$) subsystem A_2. The open-loop BACT system, through coordinate transformation matrix T_c, takes the canonical modal form

$$\dot{\mathbf{x}} = T_c A T_c^{-1}\mathbf{x}_c + T_c B u = \begin{bmatrix} A_1 & 0 \\ 0 & A_2 \end{bmatrix}_c \mathbf{x} + \begin{bmatrix} B_1 \\ B_2 \end{bmatrix}_c u = A_c \mathbf{x} + B_c u; \qquad y = C T_c^{-1}\mathbf{x} \tag{8}$$

where $A_{1c} \in R^{2\times 2}$, $A_{2c} \in R^{6\times 6}$, $B_{1c} \in R^{2\times 1}$, and $B_{2c} \in R^{6\times 1}$ are dynamic pressure-dependent submatrices of $A_c \in R^{8\times 8}$ and $B_c \in R^{8\times 1}$. In this canonical modal form, the system dynamics are expressed as two decoupled subsystems: an antistable subsystem $(A_1, B_1)_c$, with a state vector $\mathbf{x}_a = [x_1, x_2]_c^T$, and a stable subsystem $(A_2, B_2)_c$, with a state vector $\mathbf{x}_s = [x_3, x_4, x_5, x_6, x_7, x_8]_c^T$. In the remainder of this Note, the canonical modal form is assumed, and the canonical notation c will be omitted.

The antistable and stable subsystems are, respectively,

$$\dot{\mathbf{x}}_a = A_1 \mathbf{x}_a + B_1 u \tag{9}$$

$$\dot{\mathbf{x}}_s = A_2 \mathbf{x}_s + B_2 u \tag{10}$$

The 24 BACT plant models were put into the preceding canonical modal form using MATLAB's canon command. Reference [10] applied the theory of [12] to establish the semiglobal stabilizability of the higher-order ($n = 8$) BACT system in Eq. (8) under bounded control. The algorithm for bounded control of the higher-order system is detailed in [9].

A. Stabilizing State-Feedback Control

Output regulation of the full-order open-loop unstable BACT system, under saturated control, is based upon the state-feedback stabilization of its antistable planar subsystem within a bounded domain of attraction. Consider the closed-loop antistable planar subsystem

$$\dot{\mathbf{x}}_a = A_1 \mathbf{x}_a - B_1 \text{sat}(\mathbf{F}\mathbf{x}_a) \tag{11}$$

The saturation function is defined as

$$\text{sat}(\mathbf{F}_0 \mathbf{x}_a) = \text{sign}(\mathbf{F}_0 \mathbf{x}_a) \min[1, |\mathbf{F}_0 \mathbf{x}_a|] \tag{12}$$

where $\mathbf{F}_0$ is a gain vector to be determined. It has been shown that the origin is the unique equilibrium point of equation (11) [12].

The domain of attraction of the origin of Eq. (11) is defined as

$$\mathcal{S} = \{\mathbf{x}_0 \in R^2: \lim_{t\to\infty} \phi(t, \mathbf{x}_0) = 0\} \tag{13}$$

where $\phi(t, \mathbf{x}_0)$ is the unique solution of Eq. (11) for initial condition $\mathbf{x_0}$. The boundary of the domain of attraction $\partial\mathcal{S}$ is determined by the time-reversed dynamics

$$\dot{\chi}_a = -A_1 \chi + B_1 \text{sat}(\mathbf{F}_0 \chi) \tag{14}$$

of the antistable subsystem. A full description of this derivation is given in [12].

The stabilizing state-feedback control law forms the basis upon which $\mathcal{S}$ and the dynamic output regulation control law are designed. The control law is described as follows:

The state-feedback law

$$u = -\text{sat}(\mathbf{F}_0 \mathbf{x}_a) \tag{15}$$

is said to be stabilizing if the feedback matrix $[A_1 - B_1\mathbf{F}_0]$ is asymptotically stable. The feedback gain $\mathbf{F}_0$ is computed by solving the algebraic Riccati equation (ARE) for the positive definite 2×2 matrix P_1:

$$A_1^T P_1 + P_1 A_1 - P_1 B_1 B_1^T P_1 = 0 \tag{16}$$

The ARE is associated with the minimum energy cost function:

$$J = \int_0^\infty u^T(t) u(t)\, \mathrm{d}t$$

The minimum energy gain is computed as $\mathbf{F}_0 = B_1^T P_1$.

B. Null Controllable Region

For the BACT model under study, the size of the domain of attraction in Eq. (13) of the antistable subsystem depends on the choice of the stabilizing linear state-feedback control gain vector $k\mathbf{F}_0$, $k > 0.5$. More conservative estimates of domains of attraction, consisting of ellipsoids in the neighborhood of the equilibrium point, have been derived for the BACT model in [10]. The construction of conditionally large domains of attraction $\mathcal{S}(k)$ for a saturated linear control applied to the antistable subsystem (10) is derived in [12] using the concept of the null controllable region, which is defined as follows.

Consider the general linear system under saturation control

$$\dot{\mathbf{x}} = A\mathbf{x} + Bu \tag{17}$$

where $\mathbf{x} \in R^n$ and $u \in \mathcal{U}$ in Eq. (4). The null controllable region $\mathcal{C}$ of the system in Eq. (17) is defined as the set of states for which the state trajectory $\mathbf{x}(t)$ satisfies the criteria that, if $\mathbf{x}(0) = \mathbf{x}_0 \in \mathcal{C}$ and there exists an admissible control u, then there exists a time $T \in [0, \infty)$, such that $\mathbf{x}(T) = 0$. A state $\mathbf{x}_0$ is said to be asymptotically null controllable if there exists an admissible control u, such that the state trajectory $\mathbf{x}(t)$ of the system in Eq. (17) satisfies $\mathbf{x}(0) = \mathbf{x}_0$ and

$$\lim_{t\to\infty} \mathbf{x}(t) = 0$$

The asymptotically null controllable region $\mathcal{C}_a$ is a relaxation of the constraint on controllability of all poles and allows for the situation where some poles are uncontrollable and stable.

The analysis and design of feedback controllers for the BACT model can be restricted to considerations of the null controllable region of the antistable subsystem. Moreover, if (A, B) is controllable, then $\mathcal{C} = \mathcal{C}_a$. These results follow from two properties (proven in [12]):

1) If (A, B) is controllable and (A, B) is in canonical form, the set $\mathcal{C} = \mathcal{C}_1 \times \mathcal{C}^{n_2}$ denotes the null controllable region of the system in Eq. (17), where $\mathcal{C}_1$ is the null controllable region of the planar antistable subsystem in Eq. (9), and the set $\mathcal{C}^{n_2} = R^{n_2}$ denotes the null controllable region of the stable n_2-order subsystem in Eq. (10).

2) If (A, B) is stabilizable and (A, B) is in the canonical modal form, the set $\mathcal{C}_a = \mathcal{C}_1 \times \mathcal{C}^{n_2}$ denotes the asymptotically null controllable region of Eq. (17).

The preceding characterization of the null controllable region can be rephrased in terms of the reachable region $\mathcal{R}$ for the time-reversed system:

$$\dot{\chi} = -A\chi - B\upsilon \tag{18}$$

The reachable region consists of all final states χ_f of state trajectory $\chi(t)$ that are reachable at some time $T \in [0, \infty)$ for an admissible control υ and an initial state $\chi(0) = 0$. The boundary $\partial\mathcal{C}$ of the null controllable region $\mathcal{C}$ is identical with the boundary $\partial\mathcal{R}$ of the reachable region $\mathcal{R}$. This follows from the fact that the two systems in Eqs. (17) and (18) have the same curves as trajectories but traverse in opposite directions. The general characteristics and construction of the reachable region are described in [12], and the specific construction, in the case of the BACT model, for the case of complex conjugate pairs of antistable eigenvalues, is described in [10].

The following property describes the relationship between the null controllable region of the system in Eq. (17) and the domain of attraction of the origin, which is the unique equilibrium point of the system. It also establishes the semiglobal stabilization of the antistable subsystem (9) by bounded linear feedback control.

Consider the closed-loop antistable subsystem

$$\dot{\mathbf{x}}_a = A_1\mathbf{x}_a + B_1 u, \qquad u = -\text{sat}(k\mathbf{F}_0\mathbf{x}_a) \in \mathcal{U}, \qquad u, k \in R^1 \tag{19}$$

with gain $k\mathbf{F}_0$, where $\mathbf{F}_0 = B_1^T P_1$, and the positive definite matrix P_1 solves the ARE (16). It can be shown, using the infinite gain margin property of LQR regulators [21], that the origin is a stable equilibrium of Eq. (19) for $k > 0.5$. Let $\mathcal{S}(k)$ be the domain of attraction of the equilibrium $\mathbf{x} = 0$ of Eq. (19). It can also be shown [12] that

$$\lim_{k\to\infty} \text{dist}[\mathcal{S}(k), \mathcal{C}] = 0 \tag{20}$$

where dist$(\cdot)$ is the Hausdorff distance between the two sets. Moreover, the boundary of the domain of attraction $\partial\mathcal{S}(k)$ is the unique limit cycle of the planar antistable system in Eq. (19) and the time-reversed system

$$\dot{\mathbf{x}}_a = -A_1\mathbf{x}_a + B_1\text{sat}(k\mathbf{F}_0\mathbf{x}_a) \tag{21}$$

This limit cycle is a stable one for the system in Eq. (21) and an unstable one for Eq. (19). Therefore, one can determine $\partial\mathcal{S}(k)$ by simulating the time-reversed system in Eq. (21) for a given $k > 0.5$.

C. Asymptotically Regulatable Region

Consider the output regulation system in Eq. (3) and its connection to the dynamic control law in Eq. (6). The asymptotically regulatable region $\mathcal{R}_g^a$ is defined as the set of all $(\mathbf{z}_0, \mathbf{w}_0)$ for which there exists an admissible control $u(\cdot)$, such that the response of the system in Eq. (3) satisfies

$$\lim_{t\to\infty} \mathbf{z}(t) = 0$$

The regulatable region R_g is the set of all $(\mathbf{z}_0, \mathbf{w}_0)$ for which a finite time $T_{\mathbf{z}_0,\mathbf{w}_0} > 0$ exists along with an admissible control u, such that $\mathbf{z}_0 = 0$ for all $t > T$. Denote the time response $\mathbf{z}(t)$ to the initial state $(\mathbf{z}_0, \mathbf{w}_0)$ as $\mathbf{z}(t, \mathbf{z}_0, \mathbf{w}_0)$, and define

$$\mathcal{S}_{zw} := \{(\mathbf{z}_0, \mathbf{w}_0) \in R^n \times \mathcal{W}_0 \colon \lim_{t\to\infty} \mathbf{z}(t, \mathbf{z}_0, \mathbf{w}_0) = 0\}$$

$\mathcal{S}_{zw}$ is the set of initial conditions where output regulation is achieved. The set $\mathcal{S}_{zw}$ is a subset of the asymptotically regulatable region $\mathcal{R}_g^a$. A design objective is to design a control law such that $\mathcal{S}_{zw}$ is as large as possible, or as close to $\mathcal{R}_g^a$ as possible.

Assume that $V \in R^{n\times r}$ is the unique matrix solution of the generalized Lyapunov equation:

$$-AV + VS = -B\Gamma \tag{22}$$

for the coefficient matrices A, B, and S of the plant and exosystem in Eq. (3). V can be partitioned, given the canonical decomposition of the BACT model in Eq. (8), as

$$V = \begin{bmatrix} V_1 \\ V_2 \end{bmatrix} \tag{23}$$

with V_1 satisfying the equation

$$-A_1V_1 + V_1S = -B_1\Gamma \tag{24}$$

The assumption that a unique solution V exists holds when A and S have no common eigenvalues [13]. This assumption is satisfied for the output regulation problem described in the numerical example of this study. The matrix S is chosen to have imaginary eigenvalues, thus guaranteeing the uniqueness of solution matrix V. The asymptotically regulatable region $\mathcal{R}_g^a$ of the system (3) is equivalent to the cross product $\mathcal{R}_{g1} \times R^{n_2}$, where $\mathcal{R}_{g1}$ is the regulatable region of the planar antistable subsystem

$$\dot{\mathbf{z}}_1 = A_1\mathbf{z}_1 + B_1 u - B_1\Gamma\mathbf{w} \qquad \dot{\mathbf{w}} = S\mathbf{w} \tag{25}$$

Reference [13] states and proves the following relationship between the regulatable and null controllable regions:

$$\mathcal{R}_{g1} = \{(\mathbf{z}_{1_0}, \mathbf{w}_0) \in R^{n_1} \times \mathcal{W}_0 \colon \mathbf{z}_{1_0} - V_1\mathbf{w}_0 \in \mathcal{C}_1\} \tag{26}$$

The relationship between the null controllable region and the regulatable region is used in Sec. VI to define the set of points belonging to the domain of attraction $\mathcal{S}$ ($\mathcal{S} \subset \mathcal{C}_1$) for the antistable subsystem in Eq. (25) that can be embedded as a subset of $\mathcal{S}_{zw}$ for achieving the output regulation of the full eighth-order system in Eq. (3).

V. Output Regulation Control Law Design

The first step in creating a dynamic controller that solves the output regulation problem of the plant and exosystem in Eq. (3) is the construction of a continuous stabilizing feedback control law $u = f(\mathbf{v})$, $f \colon R^n \to \mathcal{U} \in R^m$ and the construction of the origin's domain of attraction $\mathcal{S}(k)$, for a suitable $k > 0.5$ of the closed-loop system

$$\dot{\mathbf{v}} = A\mathbf{v} + Bf(\mathbf{v}) \tag{27}$$

where $\mathbf{v}$ is a general n-dimensional state vector. It is assumed in this first step that $\mathcal{S}(k) \subset \mathcal{C}^a$.

The next step is the construction of a bounded invariant set $S_I \subset S(k)$ that contains the origin in its interior and guarantees that a trajectory $\mathbf{v}(t)$ of the system, subject to a bounded disturbance η,

$$\dot{\mathbf{v}} = A\mathbf{v} + Bf(\mathbf{v}) + \eta, \qquad |\eta|_\infty \le d_0 \tag{28}$$

for some positive number d_0, will go to zero under a continuous bounded control u for every $\mathbf{v}(0) \in \mathcal{S}_I$, as long as

$$\lim_{t\to\infty} \eta(t) = 0$$

In this step, it is assumed that S_I is a bounded invariant set that contains the origin in its interior. The assumptions on the existence of a stabilizing state-feedback law and an invariant set $\mathcal{S}_I$ are formally stated in [11,13].

For the open-loop BACT system in Eq. (8), construction of the state-feedback control law and the invariant set $\mathcal{S}_I$ are restricted to the planar antistable subsystem in Eq. (9), since the Hurwitz stability of matrix A_2 in Eq. (10) implies, for the stable subsystem with bounded control $(u - \Gamma\mathbf{w})$, bounded-input/bounded-output stability.

A. Construction of Invariant Set $\mathcal{S}_I$

Invariant and strictly invariant sets are the building blocks for achieving semiglobal stabilization of linear systems with saturation control. Reference [11] illustrates the construction of invariant sets for the problem of output regulation of the BACT plant and exosystem under saturation state-feedback control with additive disturbance $\Gamma\mathbf{w}$. A set in R^n is considered invariant if any trajectory of the closed-loop system under $\mathbf{w}$ starting from the set remains in it for any $\mathbf{w}$, such that $|\mathbf{w}|_2 \leq 1$ [22]. For the purpose of disturbance rejection, a small invariant set S_I containing the origin in its interior is preferred, so that a trajectory starting from a sufficiently small neighborhood of the origin will stay close to the origin.

In this section, sufficiency conditions are stated for an ellipsoid $\zeta(P, \rho)$, defined as the set $\{\mathbf{x}\colon \mathbf{x}^T P\mathbf{x} \leq \rho\}$, for a given positive definite matrix P and a scalar $\rho > 0$, to be an invariant set for the following closed-loop dynamic system with a bounded linear state-feedback control $u = F\mathbf{x}$ for some gain matrix F and bounded disturbance $\mathbf{w}$:

$$\dot{\mathbf{x}} = A\mathbf{x} - B\text{sat}(F\mathbf{x}) + E\mathbf{w} \tag{29}$$

where $-\text{sat}(\cdot)$ is the standard saturation function in Eq. (12) and E is a disturbance coefficient matrix. In the context of this study, the disturbance matrix $E = -B\Gamma$ in Eq. (3).

Specifically, for the BACT model under study and a known gain matrix F, the following theorem gives sufficiency conditions for an ellipsoid $\mathcal{S}_I = \xi(P, \rho)$ to be a (strictly) invariant set of the closed-loop system in Eq. (28).

Theorem 1 (Invariance) [22]: Assume that the bounded disturbance $\mathbf{w}$ belongs to the set

$$\mathcal{W} = \{\mathbf{w}\colon \mathbf{w}(t)^T\mathbf{w}(t) \leq 1 \quad \forall\ t \geq 0\}$$

For a given initial state $\mathbf{x}_0$ and $\mathbf{w} \in \mathcal{W}$, denote the state trajectory of the closed-loop system in Eq. (29) under $\mathbf{w}$ as $\psi(t, \mathbf{x}_0, \mathbf{w})$. For a given set $\xi(P, \rho)$ and feedback gain matrix F, if there exist an auxiliary feedback gain matrix $H \in R^{1\times n}$ and a positive number η, such that

$$\begin{aligned}&(A - BH)^T P + P(A - BH) + \tfrac{1}{\eta}PEE^T P + \tfrac{\eta}{\rho}P \leq 0(<0)\\ &(A - BF)^T P + P(A - BF) + \tfrac{1}{\eta}PEE^T P + \tfrac{\eta}{\rho}P \leq 0(<0)\end{aligned} \tag{30}$$

and

$$\xi(P, \rho) \subset \mathcal{L}(H) = \{\mathbf{x} \in R^n\colon\ -1 < H\mathbf{x} < 1\}$$

then $\xi(P, \rho)$ is a (strictly) invariant set for the system in Eq. (29). The sufficiency conditions of Theorem 1 are satisfied in the construction of the invariant set $\mathcal{S}_I$, as presented in the numerical example of this study.

B. Construction of Domain of Attraction $\mathcal{S}(k, \epsilon)$

A design objective is the boundedness of the trajectories that solve the output regulation problem for some set of initial states, where the set may be as large as possible. This requires a large domain of attraction of the equilibrium point of the closed-loop system in Eq. (27).

Section VIII presents a numerical example for which the saturation control law $f(\mathbf{v}) = -\text{sat}[k\mathbf{F}_0(\epsilon)\mathbf{v}]$ allows for a fixed disturbance $\epsilon > 0$, where $\mathbf{F}_0(\epsilon) = -B_1^T P(\epsilon)$, and $P(\epsilon)$ is the unique positive definite solution of the ARE:

$$A_1^T P(\epsilon) + P(\epsilon)A_1 - P(\epsilon)B_1B_1^T P(\epsilon) + \epsilon I = 0 \tag{31}$$

Denote the set $\mathcal{S}(k, \epsilon)$ as the domain of attraction of the origin of the antistable subsystem:

$$\dot{\mathbf{v}} = A_1\mathbf{v} - B_1\text{sat}[k\mathbf{F}_0(\epsilon)\mathbf{v}] \tag{32}$$

The domain of attraction $S(k, \epsilon)$ serves in the general analysis as an invariant set for the system in Eq. (27), such that all trajectories beginning within it are asymptotically bounded. Moreover, $S(k, \epsilon)$ is a continuous function of k and, as k increases, $S(k, \epsilon)$ moves closer to the boundary of the null controllable region.

VI. Output Regulation with State Feedback

Define

$$D_{zw} = \{(\mathbf{z}, \mathbf{w}) \in R^n \times \mathcal{W}_\mathbf{0}\colon \mathbf{z} - V\mathbf{w} \in \mathcal{S}\} \tag{33}$$

where $\mathcal{S}$ [e.g., $\mathcal{S}(k)$ for a suitable k] is the domain of attraction of the origin of the nth-order closed-loop system:

$$\dot{\mathbf{v}} = A\mathbf{v} + Bu, \qquad u = f(\mathbf{v}) \tag{34}$$

A design objective is to construct the output regulation control law in Eq. (6), such that $D_{zw} \subset \mathcal{S}_{zw}$. This would ensure that D_{zw} is a subset of the initial conditions that solve the system of output regulation equations (3). This is accomplished by an appropriate choice of stabilizing state-feedback control law $u = f(\mathbf{v})$. It would then follow, by the definition of R_{g1} in Eq. (26), that if $\mathcal{S} = \mathcal{C}^a$, then $D_{zw} = \mathcal{S}_{zw} = R_g^a$. A control law satisfying this requirement is chosen in the following manner.

Consider a simple feedback law $u = f(\mathbf{z} - V\mathbf{w})$. In [13], it is shown that D_{zw} is an invariant set for the closed-loop system

$$\dot{\mathbf{z}} = A\mathbf{z} + Bf(\mathbf{z} - V\mathbf{w}) - B\Gamma\mathbf{w} \qquad \dot{\mathbf{w}} = S\mathbf{w} \tag{35}$$

Furthermore, for all $(\mathbf{z}_0, \mathbf{w}_0) \in D_{zw}$,

$$\lim_{t\to\infty}[\mathbf{z}(t) - V\mathbf{w}(t)] = 0$$

This implies that $D_{zw} \subset \mathcal{S}_{zw}$, and $\mathbf{z}(t)$ approaches $\alpha_1(t)V\mathbf{w}$ for α_1, a continuously decreasing variable.

The dynamic state-feedback control law is stated as

$$\begin{aligned}&u = g(\alpha, \mathbf{z}, \mathbf{w}) = (1 - \alpha_1)\Gamma\mathbf{w} + \alpha_2 f\left(\frac{\mathbf{z} - \alpha_1 V\mathbf{w}}{\alpha_2}\right)\\ &\dot{\alpha}_1 = \begin{cases}0 & \text{if } \frac{\mathbf{z}-\alpha_1 V\mathbf{w}}{\alpha_2} \in \mathcal{S} \setminus \mathcal{S}_I\\ -\gamma\alpha_1 & \text{if } \frac{\mathbf{z}-\alpha_1 V\mathbf{w}}{\alpha_2} \in \mathcal{S}_I\end{cases}\\ &\dot{\alpha}_2 = \begin{cases}0 & \text{if } \frac{\mathbf{z}-\alpha_1 V\mathbf{w}}{\alpha_2} \in \mathcal{S} \setminus \mathcal{S}_I \quad \text{or } \alpha_2 \leq \delta\\ -\gamma\alpha_2 & \text{if } \frac{\mathbf{z}-\alpha_1 V\mathbf{w}}{\alpha_2} \in \mathcal{S}_I \quad \text{and} \quad \alpha_2 > \delta\end{cases}\\ &\alpha_1(0) = 1, \qquad \alpha_2(0) = 1\end{aligned} \tag{36}$$

where the parameter α_2 is introduced to prevent any possible singularities. The parameter δ is chosen to satisfy the necessary assumptions on the plant and exosystem (5). The parameter γ belongs to the interval $(0, \gamma_0]$, where γ_0 is specified as

$$\gamma_0 = \inf_{\mathbf{w}\in W_0, \mathbf{v}\in S_I} \frac{d_0}{|V\mathbf{w}|_\infty + |\mathbf{v}|_\infty} \tag{37}$$

where d_0 satisfies the conditions of Eq. (28).

The following theorem, as proven in [13], offers an efficient method for simulating the linear system in Eq. (3) with the dynamic control law in Eq. (36). This method will be demonstrated in the numerical example of the BACT model in Sec. VIII.

Theorem 2: Consider the connection of the system in Eq. (3) with the controller in Eq. (36). Let γ be chosen from the interval $(0, \gamma_0]$. Then, for all $(\mathbf{z}_0, \mathbf{w}_0) \in D_{zw}$,

$$\lim_{t\to\infty}\mathbf{z}(t, \mathbf{z}_0, \mathbf{w}_0) = 0$$

That is, $D_{zw} \subset S_{zw}$.

The numerical algorithm derived from Theorem 2 relies upon the following transformation of the closed-loop system:

$$\dot{\mathbf{z}} = A\mathbf{z} + \alpha_2 Bf\left(\frac{\mathbf{z} - \alpha_1 V\mathbf{w}}{\alpha_2}\right) - \alpha_1 B\Gamma\mathbf{w} \tag{38}$$

Letting $\mathbf{v} = (\mathbf{z} - \alpha_1 V\mathbf{w})/\alpha_2$ and assuming that V satisfies the generalized Lyapunov equation (22), the closed-loop system becomes

$$\dot{\mathbf{v}} = A\mathbf{v} + Bf(\mathbf{v}) - \left(\frac{\dot{\alpha}_1}{\alpha_2}\right)V\mathbf{w} - \left(\frac{\dot{\alpha}_2}{\alpha_2}\right)\mathbf{v} \tag{39}$$

It follows that, if $\mathbf{v}_0 \in \mathcal{S} \setminus \mathcal{S}_I$, then $\dot{\alpha}_1 = \dot{\alpha}_2 = 0$, and $\dot{\mathbf{v}} = A\mathbf{v} + Bf(\mathbf{v})$. It can be shown that, for some time t_1, $\mathbf{v}(t_1)$ will enter the invariant set $\mathcal{S}_I$ and, for $\mathbf{v}(t) \in \mathcal{S}_I$, $t \geq t_1$, the disturbance is bounded, and $\mathbf{v}(t) \to 0$ as $t \to \infty$. In the numerical example, the dynamic controller is expressed in terms of the planar antistable subsystem, where $\mathbf{z}_1$ and V_1 are solutions of Eqs. (25) and (24), respectively.

VII. Output Regulation with Error Feedback

As shown in the previous section, the basis for output regulation control law design is the stabilizing state-feedback control $u = f(\mathbf{v})$. A practical application of output regulation to aeroelastic flutter suppression requires the modification of the output regulation control law in Eq. (36) to allow for the construction of observers $(\bar{\mathbf{z}}, \bar{\mathbf{w}})$ that estimate the states $(\mathbf{z}, \mathbf{w})$ of the system when only the output response error is available for feedback.

Consider the output regulation problem of the linear system in Eq. (3). The following observer is used to reconstruct the states $\mathbf{z}$ and $\mathbf{w}$ of the nth-order system:

$$\dot{\bar{\mathbf{z}}} = A\bar{\mathbf{z}} + Bu - B\Gamma\bar{\mathbf{w}} - L_1(e - C\bar{\mathbf{z}}) \qquad \dot{\bar{\mathbf{w}}} = S\bar{\mathbf{w}} - L_2(e - C\bar{\mathbf{z}}) \tag{40}$$

where $e = C\mathbf{z}$ is the measured output response error for a reference signal $-Q\mathbf{w}$. The observer gain vector $L = [L_1{:}L_2]^T$. Letting $\tilde{\mathbf{z}} = \mathbf{z} - \bar{\mathbf{z}}$, $\tilde{\mathbf{w}} = \mathbf{w} - \bar{\mathbf{w}}$, the composite system becomes

$$\begin{aligned} \dot{\mathbf{z}} &= A\mathbf{z} + Bu - B\Gamma\mathbf{w}, \qquad \dot{\mathbf{w}} = S\mathbf{w} \\ \begin{bmatrix} \dot{\tilde{\mathbf{z}}} \\ \dot{\tilde{\mathbf{w}}} \end{bmatrix} &= \begin{bmatrix} A + L_1C & -B\Gamma \\ L_2C & S \end{bmatrix}\begin{bmatrix} \tilde{\mathbf{z}} \\ \tilde{\mathbf{w}} \end{bmatrix} \end{aligned} \tag{41}$$

Also, without loss of generality, we assume that the pair

$$(\bar{C}, \bar{A}) = \left([\,C \quad 0\,], \begin{bmatrix} A & -B\Gamma \\ 0 & S \end{bmatrix}\right) \tag{42}$$

is observable. As in the case of state feedback, it is assumed that the system matrix A consists of an antistable planar subsystem A_1 and a stable subsystem A_2 and that (A_1, B_1) is stabilizable.

Based upon the state of the observers $(\bar{\mathbf{z}}, \bar{\mathbf{w}})$, the dynamic control law is stated as [13]

$$\begin{aligned} u &= g(\alpha, \bar{\mathbf{z}}, \bar{\mathbf{w}}) = (1 - \alpha_1)\Gamma\bar{\mathbf{w}} + \alpha_2 f\left(\frac{\bar{\mathbf{z}} - \alpha_1 V\bar{\mathbf{w}}}{\alpha_2}\right) \\ \dot{\alpha}_1 &= \begin{cases} 0 & \text{if } \frac{\bar{\mathbf{z}} - \alpha_1 V\bar{\mathbf{w}}}{\alpha_2} \in S \setminus \mathcal{S}_I \\ -\gamma\alpha_1 & \text{if } \frac{\bar{\mathbf{z}} - \alpha_1 V\bar{\mathbf{w}}}{\alpha_2} \in \mathcal{S}_I \end{cases} \\ \dot{\alpha}_2 &= \begin{cases} 0 & \text{if } \frac{\bar{\mathbf{z}} - \alpha_1 V\bar{\mathbf{w}}}{\alpha_2} \in \mathcal{S} \setminus \mathcal{S}_I \quad \text{or} \quad \alpha_2 \leq \delta \\ -\gamma\alpha_2 & \text{if } \frac{\bar{\mathbf{z}} - \alpha_1 V\bar{\mathbf{w}}}{\alpha_2} \in \mathcal{S}_I \quad \text{and} \quad \alpha_2 > \delta \end{cases} \\ \alpha_1(t) &= 1, \qquad \alpha_2(t) = 1, \qquad t \in [0, T_0] \end{aligned} \tag{43}$$

where the value of T_0 is to be specified, and the decay parameter γ is defined as follows:

$$\gamma_0 = \inf_{\mathbf{w} \in W_0, \mathbf{v} \in S_I} \frac{d_0}{2(|V\mathbf{w}|_\infty + |\mathbf{v}|_\infty)} \tag{44}$$

where the parameter γ is chosen on the interval $(0, \gamma_0]$, and d_0 satisfies the conditions of Eq. (28). The parameter δ is chosen to satisfy the necessary assumptions on the plant and exosystem (5).

Let

$$\mathbf{v} = \frac{(\bar{\mathbf{z}} - \alpha_1 V\bar{\mathbf{w}})}{\alpha_2} \tag{45}$$

The closed-loop system for dynamic error-feedback control becomes

$$\begin{aligned} \dot{\mathbf{v}} = A\mathbf{v} + Bf(\mathbf{v}) - \left(\frac{\dot{\alpha}_1}{\alpha_2}\right)V\mathbf{w} - \left(\frac{\dot{\alpha}_2}{\alpha_2}\right)\mathbf{v} + \left(\frac{\dot{\alpha}_1}{\alpha_2}\right)V\tilde{\mathbf{w}} \\ - \frac{L_1 - \alpha_1 VL_2}{\alpha_2} C\tilde{\mathbf{z}} \end{aligned} \tag{46}$$

Reference [13] shows that, under the assumptions that define a saturation control law $u = f(\mathbf{v})$, an invariant set $\mathcal{S}_I$, and by the choice of L such that the estimation error is sufficiently small after T_0, and by constraints placed on the l_∞ norms of observer gains and the continuously decreasing α_1 and α_2, that the last four terms of Eq. (46) will go to zero once the trajectory $\mathbf{v}(t)$ enters the invariant set $\mathcal{S}_I$. Thus, $\mathbf{v}(t) \to 0$, and $\bar{\mathbf{z}} - \alpha_1\bar{\mathbf{w}}$, $\bar{\mathbf{z}}$, and $\mathbf{z}$ approach zero as $t \to \infty$.

The following lemma establishes the relationship between the parameter T_0 in the control law in Eq. (43) and the observer gain vector L.

Lemma 1 [13]: Denote

$$\tilde{A} = \begin{bmatrix} A + L_1C & -B\Gamma \\ L_2C & S \end{bmatrix} \tag{47}$$

Given any positive numbers T and ϵ, there exists an L such that

$$\max\{|e^{\tilde{A}t}|, |L| \cdot |e^{\tilde{A}t}|\} \leq \epsilon \quad \forall\ t \geq T \tag{48}$$

where $e^{\tilde{A}t}$ is the solution of the observer error matrix equation (41), and $|\cdot|$ is any matrix norm.

Once T_0 is chosen, based upon Lemma 1, it is possible to construct an observer vector L, such that the observer error after T_0 is as small as desired. This result enables the construction of observers, such that the performance of error-feedback control closely approximates the performance of state-feedback control. A complete in-depth derivation of the theory of output regulation with error feedback can be found in [13].

VIII. Numerical Example

This section presents an application of the underlying theory of output regulation with bounded continuous feedback control to the problem of flutter suppression, with external disturbance rejection, for BACT plant 24 and for plant models synthesized with nominal plant 24 parameters.

A. Model of Benchmark Active Control Technology System

Consider the following canonical modal state-space realization of BACT plant 24:

$$\dot{\mathbf{x}} = A\mathbf{x} + Bu + P\mathbf{w} = \begin{bmatrix} A_1 & 0 \\ 0 & A_2 \end{bmatrix}\mathbf{x} + \begin{bmatrix} B_1 \\ B_2 \end{bmatrix}u + \begin{bmatrix} P_1 \\ P_2 \end{bmatrix}\mathbf{w} \qquad y \equiv e = C\mathbf{x} = [\,C_1 \;\; : \;\; C_2\,]\mathbf{x}$$

$$A = \begin{bmatrix} A_1 & 0 \\ 0 & A_2 \end{bmatrix} = \begin{bmatrix} 1.5427 & 23.0449 & 0 & 0 & 0 & 0 & 0 & 0 \\ -23.0449 & 1.5427 & 0 & 0 & 0 & 0 & 0 & 0 \\ 0 & 0 & -4.1153 & 16.8314 & 0 & 0 & 0 & 0 \\ 0 & 0 & -16.8314 & -4.1153 & 0 & 0 & 0 & 0 \\ 0 & 0 & 0 & 0 & -14.8119 & 0 & 0 & 0 \\ 0 & 0 & 0 & 0 & 0 & -100 & 0 & 0 \\ 0 & 0 & 0 & 0 & 0 & 0 & -92.57 & 136.948 \\ 0 & 0 & 0 & 0 & 0 & 0 & -136.948 & -92.57 \end{bmatrix}$$

$$B = \begin{bmatrix} B_1 \\ B_2 \end{bmatrix} = \begin{bmatrix} -1823.51888 \\ 239.445 \\ - - - - - - - \\ 409.586 \\ -771.63679 \\ 1.549 \\ -1452878.399 \\ 1279858.07 \\ -3763625.59 \end{bmatrix} \cdot |u_{\text{sat}}|,\ |u_{\text{sat}}| = 0.4$$

$$C = [\,C_1 \;\; : \;\; C_2\,] = [\,0.6262 \quad 9.2761 \;\; : \;\; -1.6490 \quad 6.7307 \quad -5.7457 \quad -0.5345 \quad 0.59398 \quad -0.01531\,] \tag{49}$$

The eighth-order state vector $\mathbf{x}$ of the original (noncanonical) system consists of two coordinates: the BACT wing vertical displacement and pitch angle [x_1 (ft) and x_2 (rad)], their time derivative velocities [x_3 (ft/s) and x_4 (rad/s)], one aerodynamic state (x_5), and three actuator states (x_6, x_7, x_8). The control u is the hinge moment produced by the wing TE flap servoactuator. In this numerical example, its magnitude is bounded by $|u_{\text{sat}}| = 0.4$(lbf · ft). Because of the unity d.c. gain of the actuator dynamic model, this saturation value corresponds to a d.c. bound of 0.4 rad (22.9 deg) of the wing TE flap angle of deflection. To satisfy the requirements of a unity saturation function in Eq. (12), the control bounds are scaled by this saturation level, such that its normalized constraint set is $\mathcal{U} = [-1, 1]$. With $Q = 0$, in the linear matrix equations (2), $\Pi = 0$ and, in the BACT model in Eq. (49), $P = -B\Gamma$. The vector Γ is given by

$$\Gamma = [-0.3,\ 0.2,\ -0.1,\ 0.4]$$

Γ was chosen so that an invariant set $\mathcal{S}_I$ could be constructed to satisfy the assumptions placed upon it in the generalized Eq. (28) and the sufficiency conditions of Theorem 1. Applying the necessary assumption in Eq. (5) over the bounds on the additive disturbance, $|\Gamma\mathbf{w}|_\infty = 0.7722 \le \hat{\rho}\mathcal{U}$, for $\hat{\rho} = 0.8$ and $\hat{\rho} \in [0, 1)$. Hence, $\delta = 1 - \hat{\rho} = 0.2$.

The design objective is to reject the disturbance $P\mathbf{w}$, where $\mathbf{w}$ has two frequency components of 4 and 10 rad/s. That is, for the exosystem $\dot{\mathbf{w}} = S\mathbf{w}$,

$$S = \begin{bmatrix} 0 & -4 & 0 & 0 \\ 4 & 0 & 0 & 0 \\ 0 & 0 & 0 & -10 \\ 0 & 0 & 10 & 0 \end{bmatrix} \tag{50}$$

The state of the exosystem

$$\mathbf{w}(t) = [\cos(4t), \sin(4t), -\sin(10t), \cos(10t)]^T$$

The matrix A has one complex conjugate pair of antistable eigenvalues $1.5427 \pm 23.04i$. The matrices for the planar antistable subsystem are

$$A_1 = \begin{bmatrix} 1.5427 & 23.045 \\ -23.045 & 1.5427 \end{bmatrix}, \quad B_1(\text{normalized}) = \begin{bmatrix} -729.41 \\ 95.777 \end{bmatrix}$$
$$C_1 = [0.6262 \;\; 9.2761] \tag{51}$$

The state $\mathbf{z}_2 \in R^6$ of the stable subsystem

$$\dot{\mathbf{z}}_2 = A_2\mathbf{z}_2 + B_2u - B_2\Gamma\mathbf{w}, \qquad \dot{\mathbf{w}} = S\mathbf{w} \tag{52}$$

is bounded under any bounded input $u - \Gamma\mathbf{w}$. Hence, $\mathbf{z}_2(t)$ will converge to the origin as the combined input goes to zero. Therefore, one need only consider the design of feedback control laws for the antistable subsystem in Eq. (25), with the output-tracking error defined as

$$e = C_1\mathbf{z}_1 \tag{53}$$

The next step in controller design, for either state or error feedback, is to solve for V_1, the unique solution of the matrix equation

$$-A_1V_1 + V_1S = -B_1\Gamma \tag{54}$$

Matrix V_1 is used in the evaluation of the antistable subsystem's regulatable region according to the definition in Eq. (26). Solving the Lyapunov equation (54),

$$V_1 = \begin{bmatrix} 3.0676 & 0.33036 & 7.3636 & -1.9167 \\ 9.3475 & -6.8849 & 1.8405 & -15.728 \end{bmatrix} \tag{55}$$

B. Construction of State-Feedback Control Law

A stabilizing state-feedback control law $u = f(\mathbf{v})$ is constructed for the antistable system

$$\dot{\mathbf{v}} = A_1\mathbf{v} + B_1u \tag{56}$$

where the state vector $\mathbf{v} \in R^2$. For $\epsilon > 0$, let $P(\epsilon)$ be the solution of the ARE

$$A_1^TP(\epsilon) + P(\epsilon)A_1 - P(\epsilon)B_1B_1^TP(\epsilon) + \epsilon I = 0 \tag{57}$$

with the stabilizing closed-loop system gain $\mathbf{F}_0(\epsilon) = B_1^TP(\epsilon)$. Solve Eq. (57) for $\epsilon > 0$ to ensure some degree of disturbance rejection. As a result of the limiting relationship between the domain of attraction and the null controllable region (20), as $\epsilon \to 0$ and $k \to \infty$, the domain of attraction $S(k, \epsilon)$ of the origin of the system

$$\dot{\mathbf{v}} = A_1\mathbf{v} - B_1\text{sat}(\mathbf{F}_1\mathbf{v}), \qquad \mathbf{F}_1 = k\mathbf{F}_0(\epsilon) \tag{58}$$

approaches the boundary of the null controllable region $\mathcal{C}_1$ of the system in Eq. (56). Choosing $\epsilon = 0.02$ and $k = 100$, the gain is computed as

$$\mathbf{F}_1 = k\mathbf{F}_0(\epsilon) = [-13.683,\ 16.805] \tag{59}$$

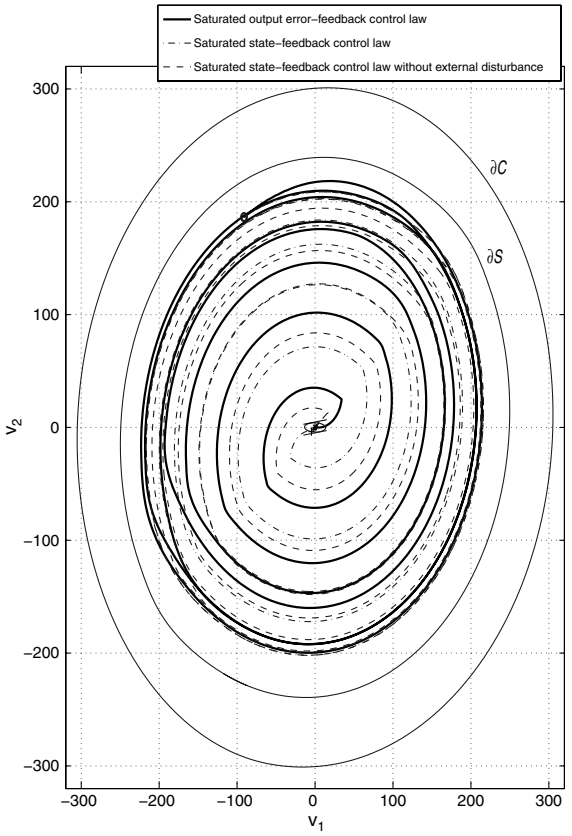

a) Antistable subsystem closed-loop trajectories

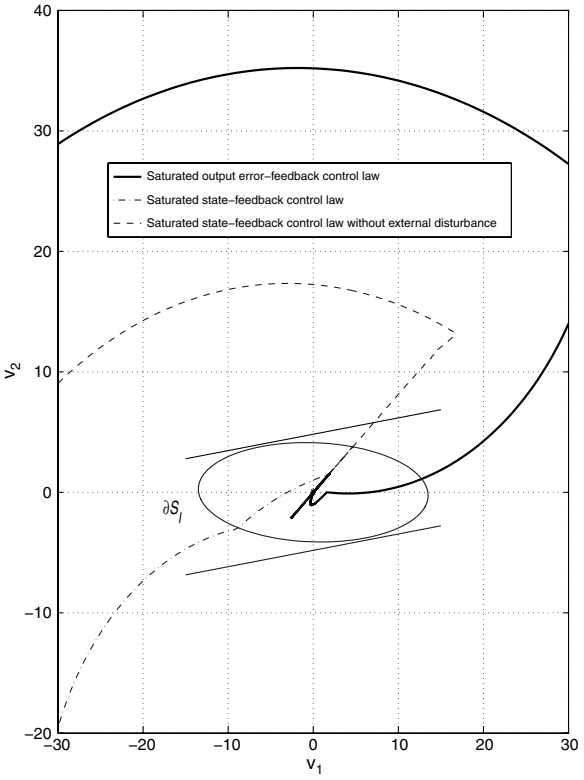

b) Trajectories entering invariant set S_I

Fig. 2 Output regulation with disturbance rejection under error feedback.

The matrix solution $P(\epsilon)$ of the ARE (57) is

$$P(\epsilon) = \begin{bmatrix} 1.929 \times 10^{-4} & 4.063 \times 10^{-5} \\ 4.063 \times 10^{-5} & 2.0641 \times 10^{-3} \end{bmatrix} \tag{60}$$

Let

$$u = f(\mathbf{v}) = -\text{sat}(\mathbf{F}_1\mathbf{v}) \tag{61}$$

Solving the inequalities in Eq. (30) of Theorem 1 (invariance) with solution matrix $P(\epsilon)$, $\eta = 0.02$, $\rho_\epsilon = 0.035$, $H = [-0.028158, 0.20748]$, and $E = B_1\Gamma$, the set

$$\mathcal{S}_I = \xi[P(\epsilon = 0.02), \rho_\epsilon] = \{\mathbf{v} \in R^2\colon \mathbf{v}^T P(\epsilon)\mathbf{v} \le \rho_\epsilon\}$$

satisfies the conditions of Theorem 1, such that $\mathcal{S}_I$ is an invariant set for the system

$$\begin{aligned} &\dot{\mathbf{v}} = A_1\mathbf{v} - B_1\text{sat}(\mathbf{F}_1\mathbf{v}) - B_1\Gamma\mathbf{w}(t), \\ &|B_1\Gamma\mathbf{w}(t)|_\infty \le d_0 = 637.21 \end{aligned} \tag{62}$$

where

$$\mathcal{S}_I \subset \mathcal{L}(H) = \{\mathbf{v} \in R^2\colon -1 < H\mathbf{v} < 1\}$$

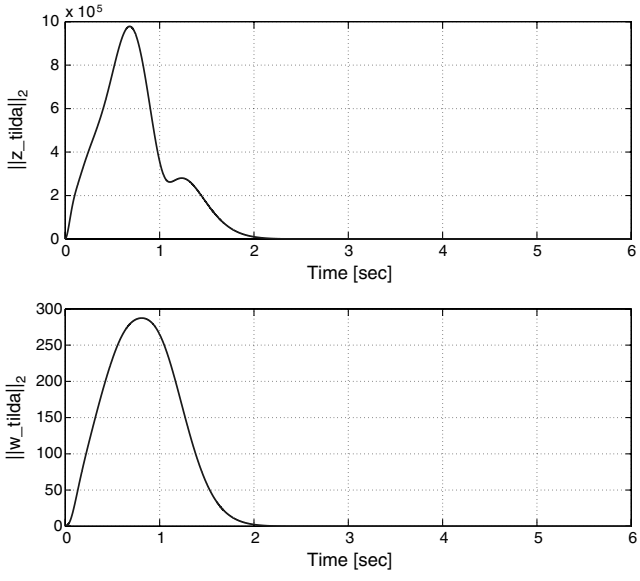

Fig. 3 $|\tilde{\mathbf{z}}|_2$ (top) and $|\tilde{\mathbf{w}}|_2$ (bottom) estimation errors.

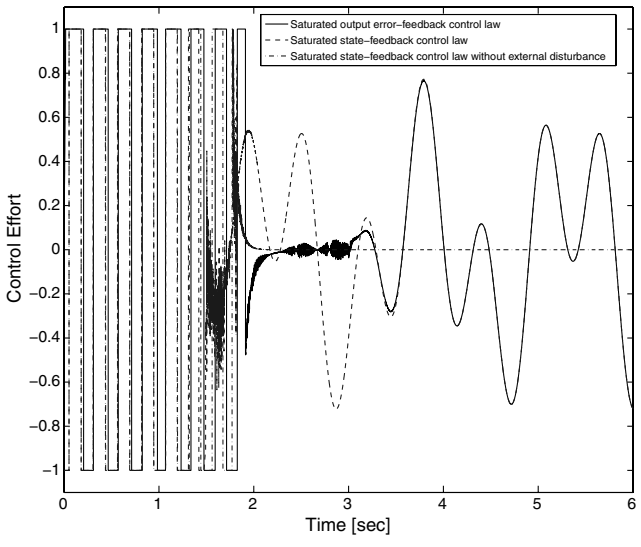

Fig. 4 Comparison of control efforts.

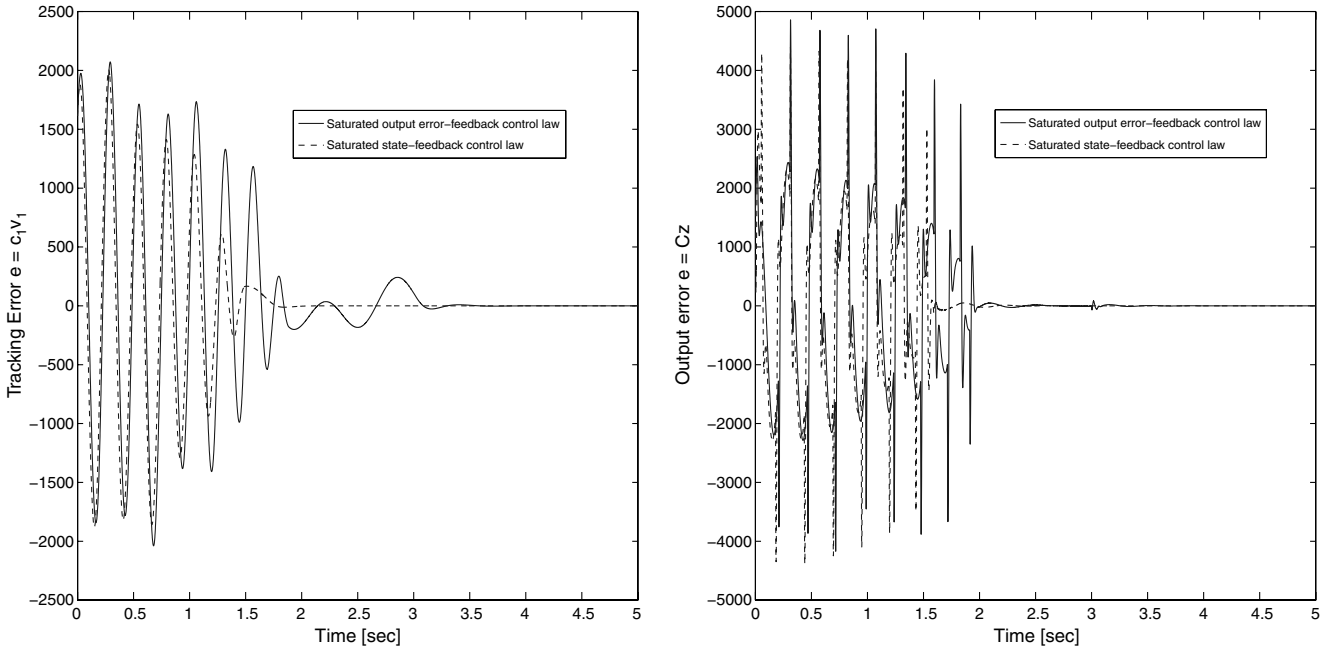

a) Antistable subsystem tracking error $e = C_1\,\mathbf{v}$ **b) Full-order system tracking error $e = C\mathbf{z}$**

Fig. 5 Tracking errors under the state- and error-feedback control laws.

Applying the definition of γ_0 in Eq. (37), the following norms are computed: $|V_1\mathbf{w}|_\infty = 33.924$ and $|\mathbf{v}|_\infty = 11.535$; the resulting $\gamma_0 = 14.017$. In the following simulations, the control parameters $\gamma = 14.0 \in (0,\ \gamma_0]$ and $\delta = 1 - \hat{\rho} = 0.2$.

For the eighth-order BACT model under study, with $\mathbf{z} = \mathbf{x} - \Pi\mathbf{w}$ and $\Pi = 0$, the initial coordinates in canonical modal form

$$\mathbf{z}\,(0) = \mathbf{x}(0) = [-90, 180, 0, 0, 0, 0, 0, 0]^T \tag{63}$$

correspond to the following initial coordinates of the original BACT system in Eq. (8):

$$\mathbf{x}^{\,b}(0) = [\,-7.9734\ \text{(ft)},\quad 0.2216\ \text{(rad)},\quad -89.296\ \text{(ft/s)},\quad 23.293\ \text{(rad/s)},\quad -4.4863 \times 10^{-3},\quad 0,\quad 0,\quad 0\,]^T$$

C. Construction of Error-Feedback Control Law

In the simulations of output regulation with error feedback, the observer gain vector L is constructed using the MATLAB place command along with the transposed matrices $(-\bar{C}^T, \bar{A}^T)$ of Eq. (42) and the following set of six pairs of complex conjugate eigenvalues p:

$$[-15 \pm 3i, -12 \pm 6i, -9 \pm 9i, -9 \pm 3i - 7.5 \pm 4.5i, -6 \pm 1.5i]$$

The observer gain vector

$$L = [\,L_1\ \ :\ \ L_2\,]^T = [\{\,-0.06361\quad -0.040372\quad 0.042067\quad 0.036751\quad -7.1456 \times 10^{-5}\quad -20.941\quad 300.44\quad 85.968\,\}:$$
$$\{\,-1.0672 \times 10^{-3}\quad 5.3047 \times 10^{-3}\quad -1.7534 \times 10^{-3}\quad 1.413 \times 10^{-3}\,\}]^T \tag{64}$$

The error estimation convergence time $T_0 = 3$ s. The decay parameter $\gamma_0 = 6.6514$ and $\gamma \in (0,\ \gamma_0]$ is set equal to 6.5. The control law is expressed as

$$u = f(\mathbf{v}) = -\text{sat}(\mathbf{F}_1\mathbf{v}), \qquad \mathbf{v}(t) = \frac{\bar{\mathbf{z}}_1 - \alpha_1 V_1 \bar{\mathbf{w}}}{\alpha_2} \tag{65}$$

D. Simulations of State- and Error-Feedback Control

In the numerical simulations of output regulation with dynamic state feedback and dynamic error feedback, the respective closed-loop systems in Eqs. (39) and (46) are expressed in terms of the antistable subsystem in Eq. (25), with the state trajectory defined as $\mathbf{v} = (\mathbf{z}_1 - \alpha_1 V_1 \mathbf{w})/\alpha_2$. Figure 2a shows the boundary of the domain of attraction $\partial\mathcal{S} \equiv \partial\mathcal{S}(k, \epsilon)$ and the boundary of the null controllable region $\partial\mathcal{C}$ for the antistable system in Eq. (56). A trajectory $\mathbf{v}$ is plotted for the closed-loop system with dynamic state feedback (dashed line) and for the closed-loop system with continuous error feedback (solid line). Figure 2a also compares these trajectories with the trajectory of the stabilizing state-feedback control law in Eq. (65) connected to the antistable subsystem in Eq. (25) and disconnected from the exosystem $\dot{\mathbf{w}} = S\mathbf{w}$ (dashed–dotted line). For the initial condition,

$$(\mathbf{z}_0, \mathbf{w}_0) = [-90, 180, 1, 0, 0, 1]D_{zw}, \mathbf{v}_0 = \mathbf{z}_0 - V_1\mathbf{w}_0$$
$$= [\,-91.15\quad 186.38\,]^T\mathcal{S}$$

The initial condition $\mathbf{v}_0$ is indicated by a circle.

Figure 2b depicts the trajectories of Fig. 2a entering the invariant set $S_I = \zeta(P(\epsilon), \rho_\epsilon)$, with $\epsilon = 0.02$ and $\rho_\epsilon = 0.035$, displayed as the solid closed ellipse. The two parallel solid straight lines in the figure indicate the boundaries of the domain of attraction of the linear feedback control: $L(H) = \{\mathbf{v} \in R^2:\ -1 < H\mathbf{v} < 1\},\ L(H) \supset S_I$. The trajectory that represents the state-feedback control (dashed line) enters the ellipse at time $t_0 = 1.476$ s, while the trajectory under error feedback (solid line) enters it at time $t_0 = 1.872$ s.

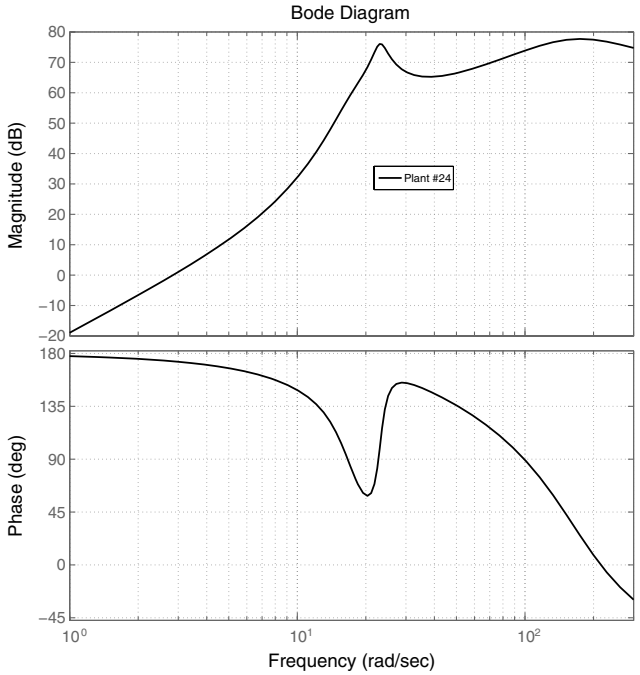

Fig. 6 Output frequency response to periodic external disturbance.

Figure 3 illustrates the l_2 norm of the observer full-order state errors $|\tilde{\mathbf{z}}|_2$ (top) and $|\tilde{\mathbf{w}}|_2$ (bottom) for output regulation using error feedback for plant 24. At $T_0 = 3$ s,

$$(|\tilde{\mathbf{z}}|_2, |\tilde{\mathbf{w}}|_2) = (11.44, 4.6 \times 10^{-3})$$

and, thereafter, the l_2 norms converge asymptotically to zero.

Figure 4 compares the control effort under output regulation for error feedback in Eq. (46) (solid line) and state feedback in Eq. (39) (dashed line) for plant 24. In addition, it compares the stabilizing state-feedback saturation control law in Eq. (65) (dashed–dotted line) for the closed-loop subsystem disconnected from the exogenous disturbance model.

Table 1 State-feedback synthesis of BACT plant antistable subsystems

Plant index	Dynamic pressure, psi	Open-loop eigenvalues	Closed-loop synthesis
24	43,805	$1.5427 \pm 23.045i$	$-20.311, -11567$
23	41,615	$1.4799 \pm 23.207i$	$-19.837, -29416$
15	24,093	$1.4799 \pm 23.207i$	$-46.17, 17530$
1	548	$-0.028553 \pm 210.18i$	$-61.036, -4316.1$

The initial phase of saturated bang–bang control behavior corresponds to the initial phase for which the trajectory $\mathbf{v} \in \mathcal{S} \setminus \mathcal{S}_I$ and $\dot{\alpha}_1 = \dot{\alpha}_2 = 0$. Satisfying these conditions, the dynamic state-feedback control law in Eq. (36) reduces to the linear saturated control

$$u = g(\alpha, \mathbf{z}, \mathbf{w}) = f(\mathbf{z} - V_1\mathbf{w}) = f(\mathbf{v})$$

Once the trajectory enters the invariant set $\mathcal{S}_I$, the parameters α_1, and α_2 decay exponentially with the decay parameter $\gamma = 14$ and α_2 bounded from below by $\delta = 0.2$. The control effort is

$$u = g(\alpha, \mathbf{z}, \mathbf{w}) = (1 - \alpha_1)\Gamma\mathbf{w} + f(\mathbf{v})$$

with $\mathbf{v} = (\mathbf{z} - \alpha_1 V_1 \mathbf{w})/\delta$. As $\mathbf{v}$ and α_1 converge to zero, the control effort converges to a nonsaturated pure external disturbance rejection control $u = \Gamma\mathbf{w}$.

The control effort for the error-feedback control law in Eq. (48) (solid line) exhibits similar qualitative behavior while delaying the exponential decay of the parameters α_1 and α_2; asymptotic convergence of the observer state estimation errors begins at $T_0 = 3$ s, as predicted by the design constraints.

Figure 5a plots the antistable subsystem tracking error $e = C_1\mathbf{v}_1$ of error-feedback (solid line) and state-feedback (dashed line) controls. Figure 5b shows the corresponding tracking error $e = C\mathbf{z}$ for the full eighth-order system for initial conditions $\mathbf{z}_0 = [-90, 180, 0, 0, 0, 0, 0, 0]^T$, $\mathbf{w}_0 = [1, 0, 0, 1]^T$, and $\alpha_0 = [1.0, 1.0]^T$. Similar regulation performance is observed for the two control laws.

E. Performance Sensitivity to External Disturbance Frequency

This section examines the sensitivity of output regulation performance to the deterministic variations of the exogenous external

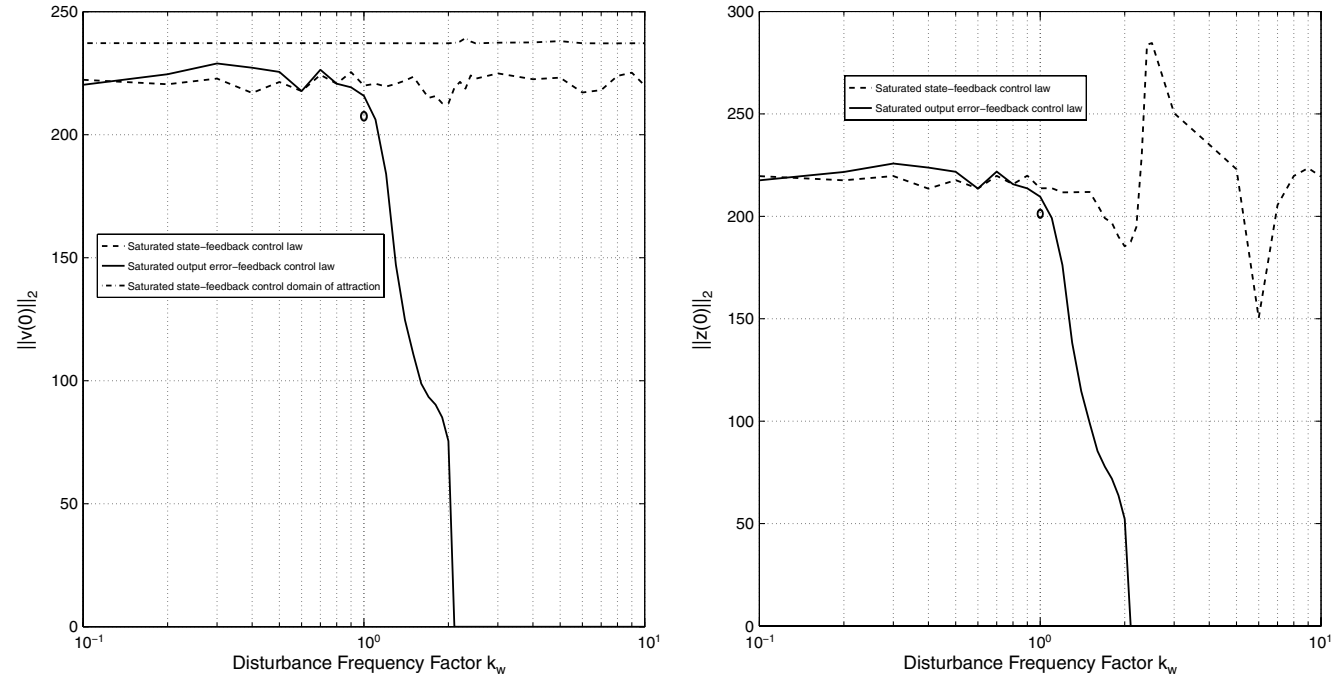

a) Max $|\mathbf{v}_0(k_w)|_2$ **b) Max $|\mathbf{z}_0(k_w)|_2$**

Fig. 7 Comparison of l_2 norms within the regulatable region $\mathcal{S}_{zw}$.

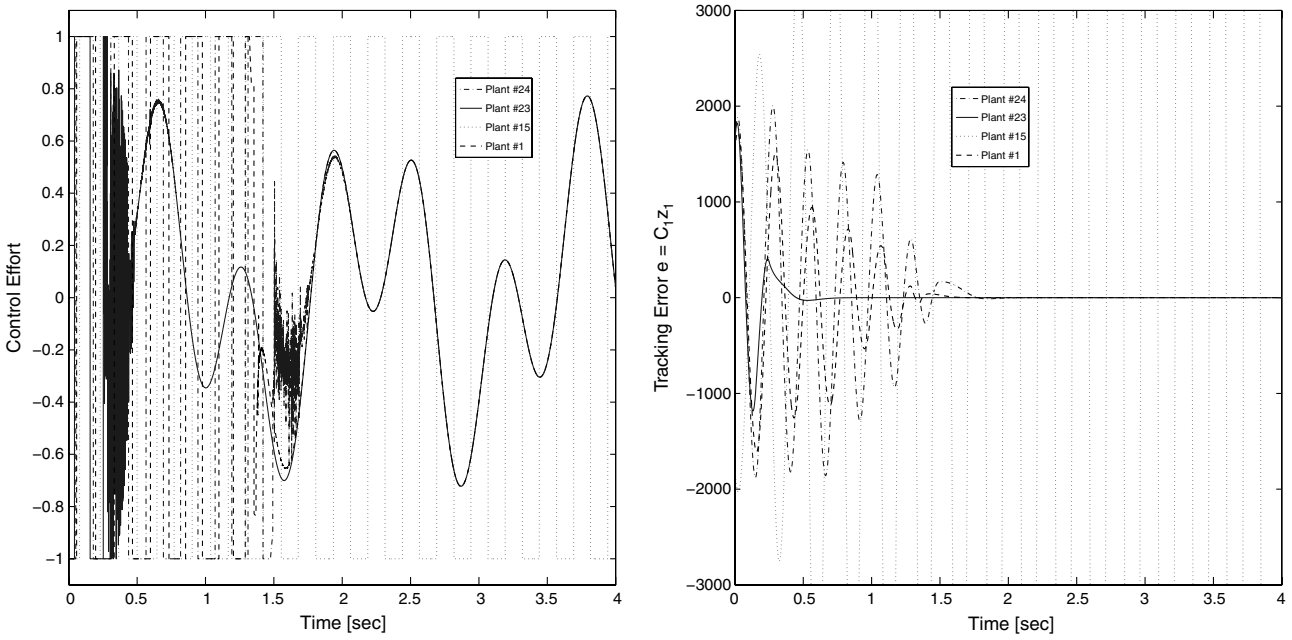

a) Comparison of control efforts **b) Comparison of tracking errors**

Fig. 8 Performance of closed-loop systems synthesized with nominal plant parameters.

periodic disturbance frequency content in Eq. (50). These variations are examined for BACT plant 24 operating under both state- and error-feedback control. According to saturated state-feedback control theory, any periodic disturbance for which the norm is bounded by $|\Gamma w|_\infty \leq \hat{\rho}$, for some $\hat{\rho} \in [0, 1)$, such that $\Gamma \mathbf{w}(t) \in \hat{\rho}\mathcal{U}$, $\forall\ t \geq 0$, can be rejected, regardless of its frequency content [13]. For the error-feedback control case, the situation becomes more complex, since the estimation errors $\tilde{\mathbf{z}}$ and $\tilde{\mathbf{w}}$ of the full-order composite system in Eq. (41) should be bounded. For an observable system, an asymptotically stable observer gain vector L can always be found. However, due to the composite closed-loop system's initial estimation error's dynamic amplification effect, which occurs for disturbances with frequency content close to or above the system's aeroelastic resonance frequency, the system's closed-loop response may exceed the boundary $\mathcal{S}_{zw}$ of the system's regulatable region, and hence finally diverge.

Figure 6 depicts the frequency response of the full-order open-loop plant's acceleration output to the periodic external disturbance input for $\Gamma = [-0.3,\ 0.2,\ -0.1,\ 0.4]$ and $\mathbf{w}_0 = [1,\ 0,\ 0,\ 1]^T$.

Because of its acceleration output, the open-loop plant exhibits high-pass filter characteristics, with a dominant lightly damped aeroelastic resonance frequency located at 23.1 rad/s, corresponding to the plant's antistable complex pole at $s = 1.5427 \pm 23.045i$.

Figure 7 examines the performance sensitivity of the closed-loop system to the external disturbance's relative frequency content. Numerical simulations determine the l_2 norm of the boundary $\partial\mathcal{S}_{zw}$

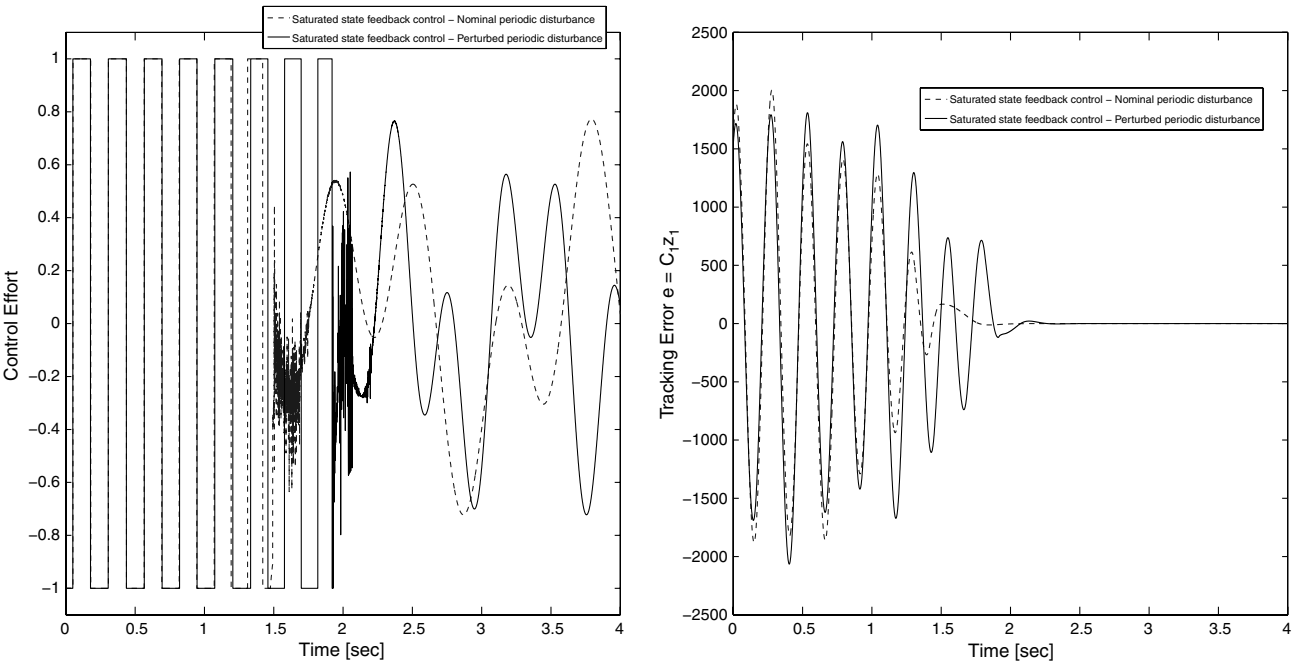

a) Comparison of control efforts **b) Comparison of tracking errors**

Fig. 9 Comparison of performance of plant 24 with disturbance matrices S_N and $1.6S_N$.

of the antistable subsystem's asymptotically regulatable region, $\partial\mathbf{v}_0(k_w) = \partial[\mathbf{z}_0 - V_1(k_w)\mathbf{w}_0]$, as a function of the disturbance frequency content, using the state-feedback gain $\mathbf{F}_1$ in Eq. (59) and the initial condition $\mathbf{w}_0 = [1, 0, 0, 1]^T$. The nominal disturbance state matrix S [Eq. (50)] was multiplied by k_w, which varied in the range $0.1 \leq k_w \leq 10$. Figures 7a and 7b compare l_2 norms for state-feedback and error-feedback controls as a function of the external disturbance relative frequency content factor k_w. Figure 7a depicts the maximum l_2 norm of $\mathbf{v}_0(k_w)$, for which the system achieves output regulation using state-feedback (dashed line) and error-feedback (solid line) controls. This is equivalent to the l_2 norm of $\partial\mathcal{S}_{zw}$. The l_2 norm of $\partial\mathcal{S} = \partial\mathcal{S}(k, \epsilon)$ (dashed–dotted line) is also shown in the figure. The circle denotes the nominal simulation value $|\mathbf{v}_0(k_w = 1)|_2$. Figure 7b depicts the corresponding $\max|\mathbf{z}_0(k_w)|_2$ graphs, where $\mathbf{z}_0 = \mathbf{v}_0 + V_1(k_w)\mathbf{w}_0(=\mathbf{x}_0)$. The figures indicate that the regulatable region for state-feedback control is insensitive to the frequency content of the external disturbance, while the regulatable region for error-feedback control diminishes to zero for disturbance with frequency content close to or above the system's aeroelastic resonance frequency.

F. Robust Performance Considerations

This section examines the robustness of output regulation relative to unmodeled system parameter variations. Because of modeling uncertainties, and due to variation of BACT open-loop dynamics with airflow dynamic pressure, precise knowledge of the system plant and the external disturbance parameters cannot be assumed.

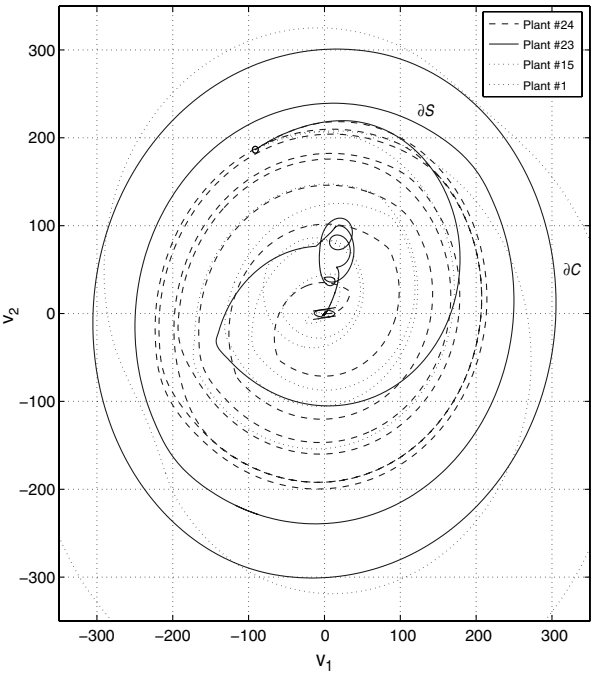

a) Antistable subsystem closed-loop trajectories

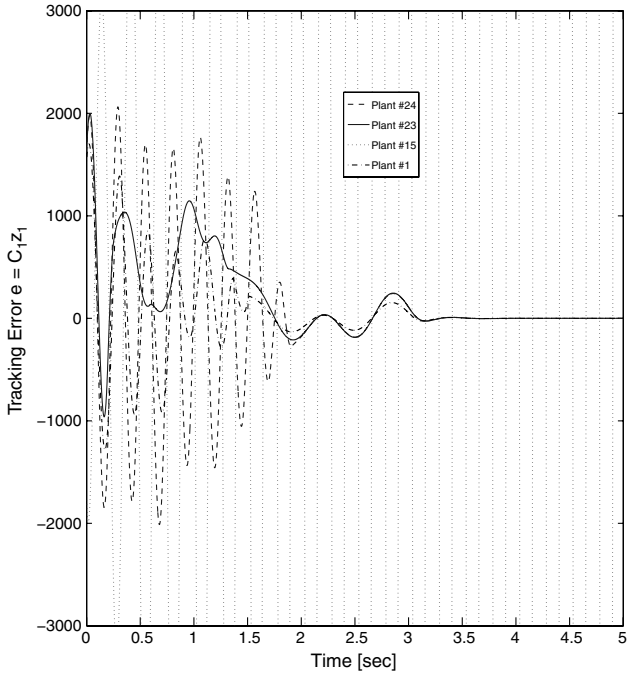

b) Antistable subsystem tracking errors $e_1 = C_{1_R}z_{1_R}$

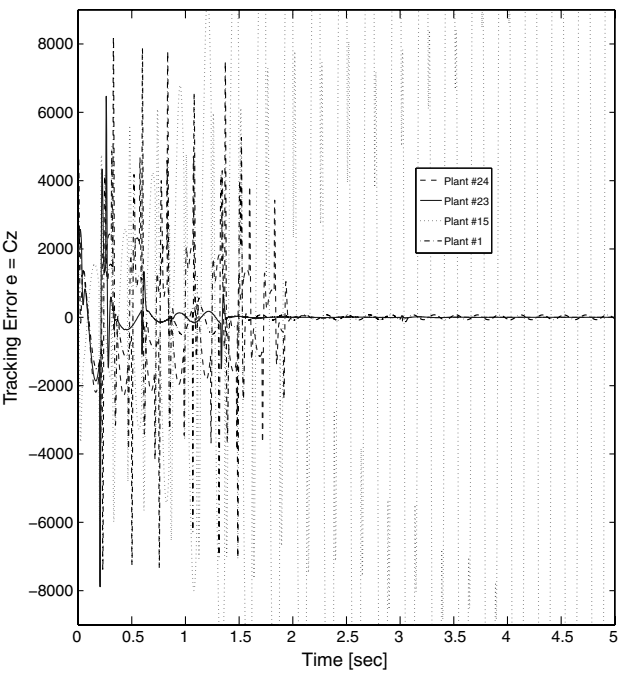

c) Full system tracking errors $e = C_R z_R$

Fig. 10 Plants 24, 23, 15, and 1 closed-loop trajectories and tracking errors under nominal control and estimation parameters.

Numerical simulations demonstrate the degrees of robustness for both state feedback and error feedback. The control parameters used in the synthesis of the worst-case nominal plant 24 are applied to a variety of other working setpoints: plants 23 and 15 (open-loop unstable) and plant 1 (open-loop marginally stable). We also examine the effect of unknown multiplicative perturbation of the external disturbance frequency content on the regulation performance of plant 24.

1. State-Feedback Synthesis

Linear state-feedback stabilization is a necessary condition for saturated control regulation. Table 1 details the open-loop and closed-loop eigenvalues of antistable subsystems for BACT plants 24, 23, 15, and 1. The eigenvalues are ordered by descending dynamic pressure setpoints, as obtained by applying the linear state-feedback gain vector $\mathbf{F}_1$ in Eq. (59), synthesized for the nominal plant 24. One can see that, for the nearest high dynamic pressure and the lowest dynamic pressure setpoints, 23 and 1, respectively, we obtain highly stable and damped closed-loop linear subsystems while, for the medium-range dynamic pressure setpoint 15, we get a highly unstable closed-loop subsystem. These results are reasonable, since no robustness considerations were taken into account while synthesizing $\mathbf{F}_1$.

Figure 8 compares the control efforts (Fig. 8a) and the tracking errors $e = C_1\mathbf{z}$ (Fig. 8b) of the antistable closed-loop synthesis of plants 1, 15, and 23 with the nominal plant 24 parameters that are described in Secs. VIII.A and VIII.B.

These parameters include the state-feedback gain vector $\mathbf{F}_1$ and the parameters that describe the invariant ellipse $\mathcal{S}_I$: the matrix solution $P(\epsilon)$ of the ARE (57), V_1, the solution of the Lyapunov equation (54), and the parameters $\epsilon = 0.02$ and $\rho_\epsilon = 0.035$. The initial conditions of the output regulation problem, $\mathbf{z}(0) \equiv \mathbf{x}(0)$ and $\mathbf{w}(0)$, are also preserved. Figure 8b describes the closed-loop stable and asymptotic convergent behaviors of plants 24, 23, and 1 with respect to their tracking errors under state feedback. Plants 24 and 1 have similar closed-loop dynamic response, while plant 23 is considerably more stable and damped. The trajectory $\mathbf{v}_a(t)$ of plant 23's antistable subsystem enters the invariant set $\mathcal{S}_I$ at 0.354 s, while the entrance times of plants 1 and 24 are 1.322 and 1.476 s, respectively. One can also observe that the marginally open-loop unstable plant 15 is not stabilized under the nominal plant 24 state-feedback control parameters, as has already been predicted by the preceding linear analysis.

The next set of simulations examines the robustness of output regulation under state feedback of plant 24 as it relates to the frequency content perturbation of the external periodic disturbance $\mathbf{w}(t)$. Nominal control parameters, including matrix $V_1(S)$ in Eq. (55), based on the nominal S matrix in Eq. (50), are used in the simulations described in Fig. 9. The closed-loop control effort (Fig. 9a) and tracking error (Fig. 9b) are depicted for the cases of a matched external disturbance frequency content $S_N = S$ (dashed line) and of an unmatched disturbance with $S_P = 1.6S_N$ (solid line). The figure shows that, up to the upper limit of the unmatched multiplicative perturbation matrix S_P, the state-feedback regulator with the nominal bounded control parameters stabilizes and regulates the system output, accompanied by a small delay in the time of entrance into the invariant set $\mathcal{S}_I$. The closed-loop control signal asymptotically cancels the actual measured external disturbance effect $\Gamma\mathbf{w}(t)$. For a higher level of unmatched frequency content perturbation, the closed-loop system is not regulatable with these nominal control parameters and initial conditions due to the unmatched matrix $V_1(S_N)$.

2. Error-Feedback Synthesis

Error-feedback synthesis consists of using the nominal models of the plant and exosystem in the observer equations (45) for reconstruction of their full-order state vectors. This is in contrast to the state-feedback case, in which the actual states of the system and exosystem are available for feedback. Let N and R indices represent the nominal and the real plant and exosystem under consideration, respectively. Assume that disturbance matrices S and Γ are the nominal parameters that have been previously defined, and let a

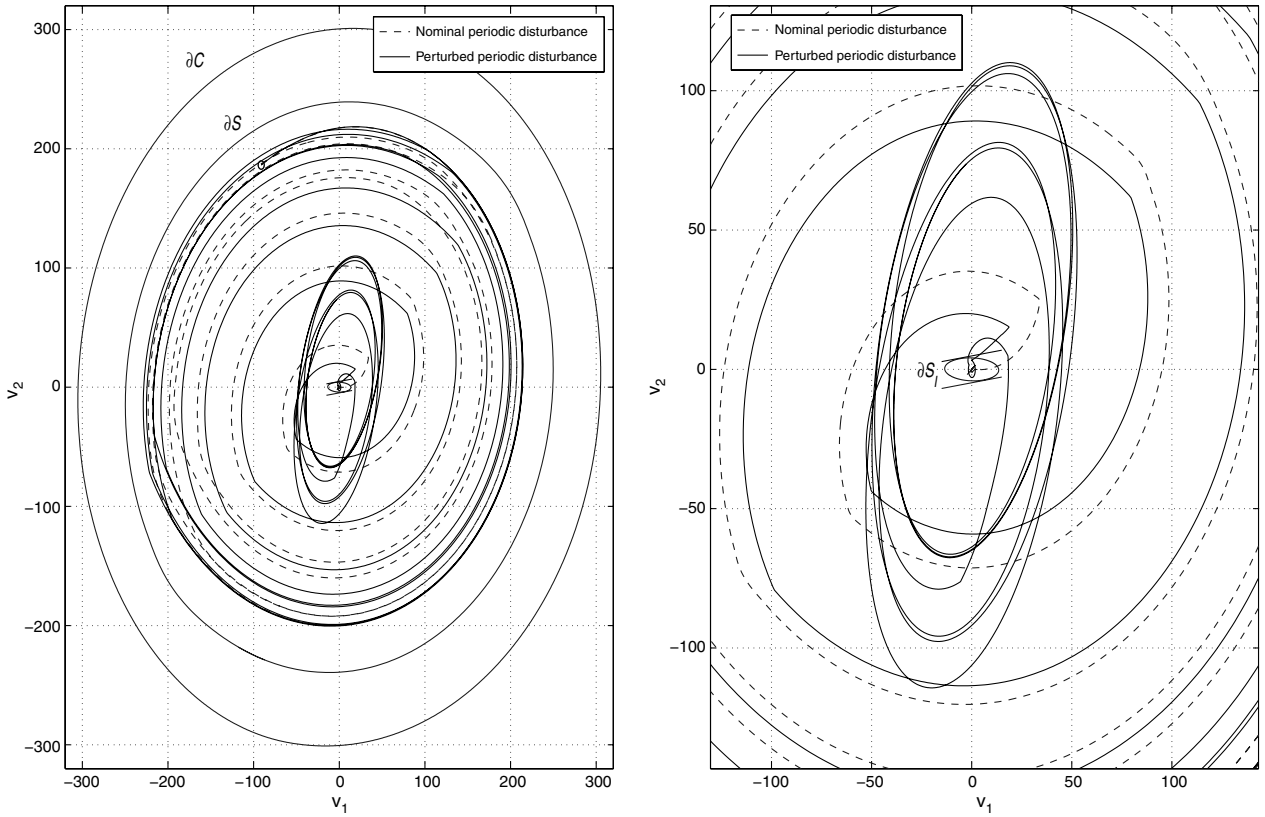

a) Trajectories for S_N and 1.1 S_N **b) Trajectories entering invariant set S_I**

Fig. 11 Plant 24 antistable subsystem closed-loop trajectories for nominal disturbance matrix S_N and for perturbed matrix $S_R = 1.1S_N$.

represent the state vector of the antistable subsystem. The equations for control synthesis under error feedback of the real plant based upon the nominal system parameters are as follows:

Denote

$$\bar{\mathbf{v}}_{a_N} = \frac{(\bar{\mathbf{z}}_{a_N} - \alpha_1 V_{1_N} \bar{\mathbf{w}}_N)}{\alpha_2}$$

$$u_N = g(\alpha, \bar{\mathbf{z}}_N, \bar{\mathbf{w}}_N) = (1-\alpha_1)\Gamma\bar{\mathbf{w}}_N + \alpha_2 f(\bar{\mathbf{v}}_{a_N}) \tag{66}$$

where $f(\bar{\mathbf{v}}_{a_N}) = -\text{sat}(F_{1_N}\bar{\mathbf{v}}_{a_N})$. The full nth-order system nominal plant observers are constructed as

$$\dot{\bar{\mathbf{z}}}_N = A_N\bar{\mathbf{z}}_N + B_N(u_N - \Gamma\bar{\mathbf{w}}_N) - L_{1_N}(e - C_N\bar{\mathbf{z}}_N)$$
$$\dot{\bar{\mathbf{w}}}_N = S\bar{\mathbf{w}}_N - L_{2_N}(e - C_N\bar{\mathbf{z}}_N) \tag{67}$$

where $e = C_R\mathbf{z}_R$. The equations for the reconstructed states are

$$\dot{\mathbf{z}}_R = A_R\mathbf{z}_R + B_R(u_N - \Gamma\mathbf{w}_R); \qquad \mathbf{z}_R(0) = \mathbf{z}_0$$
$$\dot{\mathbf{w}}_R = S\mathbf{w}_R; \qquad \mathbf{w}_R(0) = \mathbf{w}_0 \tag{68}$$

Figure 10a shows the closed-loop trajectories $\mathbf{v}_a(t)$ of the antistable subsystem under error feedback of the following BACT plants: 24 (dashed–dotted line), 23 (solid line), 15 (dotted line), and 1 (dashed line), using plant 24 nominal control and estimation parameters and observer dynamic model. The state-feedback gain $\mathbf{F}_1$ is given by Eq. (59), and the observers gains L are given by Eq. (64). The set $\mathcal{S}_I$ remains invariant under error-feedback synthesis of plant 24 parameters. The convergence time parameter of the control estimation error is $T_0 = 3$ s. In these simulations, the external disturbance matrix S is the nominal one, given by Eq. (50). Initial conditions for the eighth-order error-feedback synthesis are the same as detailed in Eq. (63). Figures 10b and 10c show the corresponding antistable subsystem closed-loop tracking error, $e_1 = C_{1_R}\mathbf{z}_{1_R}$, and the full system tracking error, $e = C_R\mathbf{z}_R$, respectively. One can observe the similarity between the closed-loop dynamic response for these various plants under error feedback and their corresponding response under state feedback in Fig. 8. The major difference is the slower tracking error convergence obtained under error feedback for the closed-loop stable plants 24, 23, and 1, due to the initial estimation error's convergence phase. One can also observe, prior to convergence, the initial nonasymptotic dynamic response of plant 23.

The final set of simulations describes robustness characteristics for the output regulation of plant 24 under error feedback for a nonnominal unmatched model of the external disturbance frequency content. Figure 11 shows the closed-loop trajectories of the antistable subsystem for the nominal disturbance matrix $S_N = S$ in Eq. (50) (dashed line) and for a slightly mismatched multiplicatively perturbed frequency disturbance matrix $S_R = 1.1S_N$ (solid line). Figure 11b shows that, for the unmatched frequency content perturbation case, the set $\mathcal{S}_I$ is no longer invariant with respect to a trajectory starting within the domain of attraction $\mathcal{S} \equiv S(k, \epsilon)$. The closed-loop trajectory $\mathbf{v}(t, \mathbf{v}_0, \mathbf{w}_0)$ approaches, at first, the origin and, for a short time period, it also enters the ellipsoid $\mathcal{S}_I$, but it finally converges into a stable periodic limit cycle outside the ellipsoid. This asymptotic periodic limit cycle response exists for any level of unmatched multiplicative frequency content perturbation under error-feedback control, up to this small upper limit value S_R. For a perturbation greater than S_R, the closed-loop system is unstable. Figure 12 shows the corresponding effect on the control effort (Fig. 12a) and tracking error (Fig. 12b).

IX. Conclusions

This study deals with flutter suppression and output regulation under bounded control for the nonminimum phase aeroelastic BACT model. Previous work demonstrated the construction of the system's domain of attraction and a continuous stabilizing state-feedback control law for achieving this goal. This Note extends previous work to the more practical case of closed-loop flutter suppression and output regulation by presenting the theory and synthesis of a saturated dynamic error-feedback control law. This control law is based on real-time estimation of the full-order state vectors of the system plant and the additive exosystem disturbance. Using a linear observer, the asymptotic closed-loop performances of the error-feedback system can be made arbitrarily close to those achieved through state feedback. The core of the dynamic control law for output regulation is the construction of two invariant sets: the domain of attraction $\mathcal{S}$ and the invariant set $\mathcal{S}_I$. The domain of attraction $\mathcal{S}$ produces bounded trajectories in an arbitrarily large subset of the null controllable region. The invariant set $\mathcal{S}_I$ can be made small enough to produce satisfactory convergence time characteristics and guarantee the continuous behavior of the control law in an arbitrarily small neighborhood of the origin. Numerical simulations of several plant models have demonstrated a similarity in output regulation

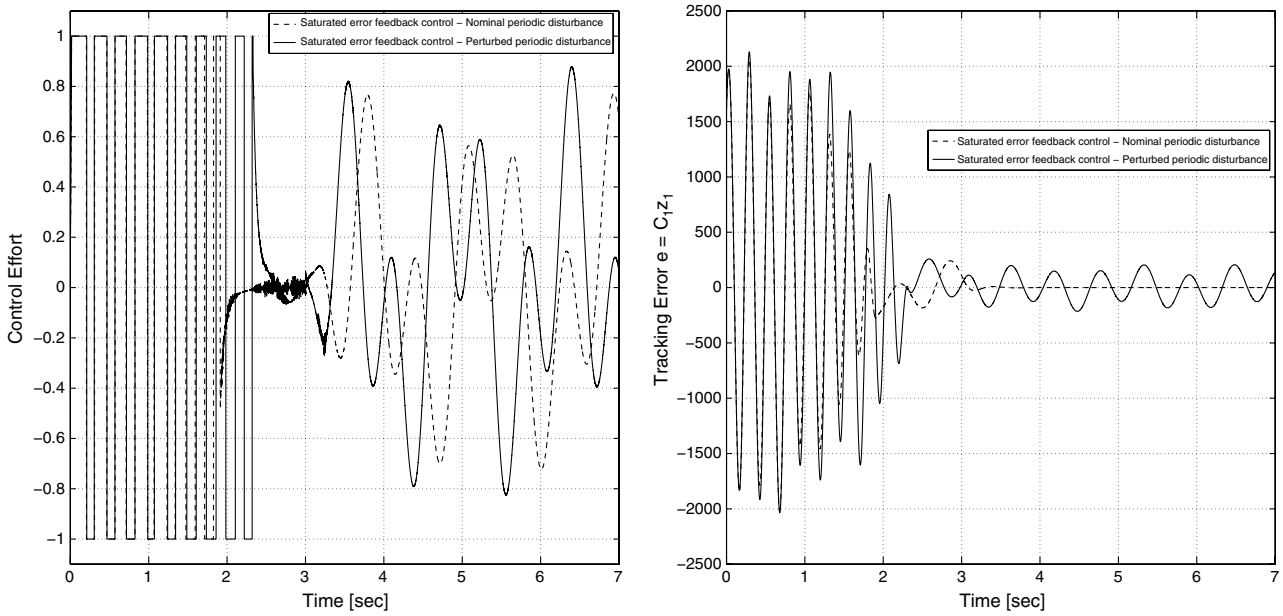

a) Comparison of control efforts **b) Comparison of tracking errors**

Fig. 12 Plant 24 closed-loop performance under nominal error-feedback estimation and control parameters with disturbance matrices S_N and $1.1S_N$.

performances between dynamic state-feedback and error-feedback control laws that were synthesized for the system's most open-loop unstable working setpoint, at the highest considered airflow dynamic pressure. Numerical simulations also demonstrate the sensitivity of the proposed error-feedback control law to the system's external periodic disturbance frequency content. For disturbances with low-relative-frequency content, the regulatable region is similar under both state-feedback and error-feedback control. However, as the disturbance frequency content approaches and exceeds the system's aeroelastic resonance frequency, the size of the regulatable region under the state-feedback control law is preserved, while for the error-feedback control law, the regulatable region shrinks to zero. This is due to the amplification effect of the exosystem's state estimation error that occurs in the case of relatively high-external-frequency disturbance.

Several issues in robustness were examined via numerical simulations. Both state-feedback and error-feedback control laws provided a similar measure of robustness to the variation of plant dynamics with the airflow dynamic pressure. These simulations were conducted using the nominal state-feedback controller and parameters and the observer dynamic model, synthesized for the most unstable open-loop BACT plant setpoint. The regulation performances of the bounded state-feedback control law, using the nominal control parameters, were found to be relatively robust to perturbation of the external disturbance frequency content. On the other hand, even small unmodeled frequency perturbations of the external disturbance content produce an oscillatory output response under the bounded error-feedback control law, which becomes closed-loop unstable for an unmatched frequency multiplication factor of only 1.1. An avenue of further investigation is the potential enhancement of the system's closed-loop robustness under error-feedback control by using the more robust Kalman filter, instead of the pole-placement-based linear observer applied in this Note. Such a filter may also be used for online identification of some uncertain system parameters: in particular, the external disturbance frequency content. A different direction is the extension of robust state-feedback time-varying sliding mode control to the more practical case of output regulation under error feedback.

Acknowledgments

The second and third authors gratefully acknowledge the financial support for this research provided by Shlomit Gali, Israel Ministry of Defense (MAFAT). The authors acknowledge the anonymous reviewers for their constructive comments that have made a considerable contribution to the quality of the content and presentation of this Note.

References

[1] Waszak, M. R., "Robust Multivariable Flutter Suppression for Benchmark Active Control Technology Wind-Tunnel Model," *Journal of Guidance, Control, and Dynamics*, Vol. 24, No. 1, Jan.–Feb. 2001, pp. 147–153. doi:10.2514/2.4694

[2] Scott, R., Hoadley, S. T., Wieseman, C., and Durham, M. H., "Benchmark Active Controls Technology Model Aerodynamic Data," *Journal of Guidance, Control, and Dynamics*, Vol. 23, No. 5, Sept.–Oct. 2000, pp. 914–921. doi:10.2514/2.4632

[3] Mukhopadhyay, V., "Transonic Flutter Suppression Control Law Design and Wind-Tunnel Test Results," *Journal of Guidance, Control, and Dynamics*, Vol. 23, No. 5, Sept.–Oct. 2000, pp. 930–937. doi:10.2514/2.4635

[4] Kelkar, A. G., and Joshi, S. M., "Passivity-Based Control with Application to Benchmark Active Controls Technology Wing," *Journal of Guidance, Control, and Dynamics*, Vol. 23, No. 5, Sept.–Oct. 2000, pp. 938–947. doi:10.2514/2.4636

[5] Barker, J., and Balas, G., "Comparing Linear Parameter-Varying Gain-Scheduled Control Techniques for Active Flutter Suppression," *Journal of Guidance, Control, and Dynamics*, Vol. 23, No. 5, Sept.–Oct. 2000, pp. 948–955. doi:10.2514/2.4637

[6] Adin, Z., Ben-Asher, J. Z., Cohen, K., Moulin, B., and Weller, T., "Flutter Suppression Using Linear Optimal and Fuzzy Logic Techniques," *Journal of Guidance, Control, and Dynamics*, Vol. 26, No. 1, 2003, pp. 173–177. doi:10.2514/2.5030

[7] Applebaum, E., Ben-Asher, J. Z., and Weller, T., "Fuzzy Gain Scheduling for Flutter Suppression in an Unmanned Aerial Vehicle," *Journal of Guidance, Control, and Dynamics*, Vol. 28, No. 6, 2005, pp. 1123–1130. doi:10.2514/1.12662

[8] Bernstein, D., and Michel, A., "A Chronological Bibliography on Saturating Actuators," *International Journal of Robust and Nonlinear Control*, Vol. 5, No. 5, 1995, pp. 375–380. doi:10.1002/rnc.4590050502

[9] Bhoir, N., and Singh, S., "Control of Unsteady Aeroelastic System via State-Dependent Riccati Equation Method," *Journal of Guidance, Control, and Dynamics*, Vol. 28, No. 1, Jan.–Feb. 2005, pp. 78–84. doi:10.2514/1.6590

[10] Applebaum, E., and Ben-Asher, J. Z., "Control of an Aeroelastic System with Actuator Saturation," *Journal of Guidance, Control, and Dynamics*, Vol. 30, No. 2, 2007, pp. 548–556. doi:10.2514/1.20763

[11] Applebaum, E., and Ben-Asher, J. Z., "Output Regulation with Bounded Control for the Benchmark Active Control Technology Model," AIAA Guidance, Navigation, and Control Conference and Exhibit, AIAA Paper 2006-6422, Aug. 2006.

[12] Hu, T., and Lin, Z., *Control Systems with Actuator Saturation, Analysis and Design*, Birkhauser, Boston, 2001.

[13] Hu, T., and Lin, Z., "Output Regulation of Linear Systems With Bounded Continuous Feedback," *IEEE Transactions on Automatic Control*, Vol. 49, No. 11, 2004, pp. 1941–1953. doi:10.1109/TAC.2004.837591

[14] Gokcek, C., Kabamba, P., Meerkov, S., and Lin, Z., "An LQR/LQG Theory for Systems with Saturating Actuators," *IEEE Transactions on Automatic Control*, Vol. 46, No. 10, 2001, pp. 1529–1542. doi:10.1109/9.956049

[15] Corradini, M., and Orlando, G., "Linear Unstable Plants with Saturating Actuators: Robust Stabilization by a Time Varying Sliding Surface," *Automatica*, Vol. 43, No. 1, 2007, pp. 88–94. doi:10.1016/j.automatica.2006.07.018

[16] Francis, B. A., "The Linear Multivariable Regulator Problem," *SIAM Journal on Control and Optimization*, Vol. 15, No. 3, 1977, pp. 486–505. doi:10.1137/0315033

[17] Isidori, A., "Output Regulation of Nonlinar Systems," *IEEE Transactions on Automatic Control*, Vol. 35, No. 2, 1990, pp. 131–140. doi:10.1109/9.45168

[18] Adin, Z., and Ben-Asher, J., "Updated BACT Aeroelastic Model-Robust Stabilization Via Various LQG Regulator Types," Faculty of Aerospace Engineering, Technion–Israel Inst. of Technology, Haifa, Israel, July 2002.

[19] Andrew, R. T., "A Nonlinear Small Gain Theorem for the Analysis of Control Systems with Saturation," *IEEE Transactions on Automatic Control*, Vol. 41, No. 9, Sept. 1996, pp. 1256–1270. doi:10.1109/9.536496

[20] Farrell, J., Sharna, M., and Polycarpou, M., "Backstepping-Based Flight Control with Adaptive Function Approximation," *Journal of Guidance, Control, and Dynamics*, Vol. 28, No. 6, Nov.–Dec. 2005, pp. 1089–1102. doi:10.2514/1.13030

[21] Anderson, B., and Moore, J., *Linear Optimal Control*, Prentice–Hall, Englewood Cliffs, NJ, 1971, pp. 70–77, Chap. 5.

[22] Hu, T., Lin, Z., and Chen, B. M., "An Analysis and Design Method for Linear Systems Subject to Actuator Saturation and Disturbance," *Automatica*, Vol. 38, No. 2, 2002, pp. 351–359. doi:10.1016/S0005-1098(01)00209-6